DEVELOPMENT OF 2-D AND 3-D PAPER-BASED MICROFLUIDIC DEVICES FOR THE DETECTION OF CRYPTOSPORIDIUM AND GIARDIA

by

Shalini Madadi, B.S.

A thesis submitted to the Graduate Council of
Texas State University in partial fulfillment
of the requirements for the degree of
Master of Science
with a Major in Biology
May 2015

Committee Members:

Shannon E. Weigum, Chair.

Robert McLean.

Rodney E. Rohde.

FAIR USE AND AUTHOR'S PERMISSION STATEMENT

Fair Use

Duplication Permission

ACKNOWLEDGEMENTS

I would like to thank all of those who were with me at every step of my life helping me and guiding me, my parents and my husband Sid for making me the person I am today and support me since the day I was in their life. Special thanks to my advisor and mentor, Dr. Shannon Weigum, who supported me and guided me towards finishing my master's degree and also in my personal life, without her I wouldn't have reached where I am now. I have learnt many things from her, like experimental designing, presentation, organization, etc that I will cherish forever. This thesis was submitted to the committee for final review on December 17th, 2014.

TABLE OF CONTENTS

Page

LIST OF TABLES

Table **Page**

LIST OF FIGURES

Figure **Page**

LIST OF ABBREVIATIONS

Abbreviation	Description
2-D	2- dimensional
3-D	3- dimensional
AP	Alkaline phosphatase
CA	Cellulose acetate
C zone	Control zone
DIA	Direct immunoassay
EIA	Enzyme immunoassay
ELISA	Enzyme-linked immunosorbent assay
GB	Guardian buffer
HRP	Horse-raddish peroxidase
NBT/BCIP	Nitro-blue tetrazolium and 5-bromo-4-chloro-3'-indolyphosphate
ORT	Oral rehydration therapy
PC	Polycarbonate
PCR	Polymerase chain reaction
POC	Point-of-care
ROI	Region of interest
RT	Room temperature
TB	Tuberculosis
TMB	Tetramethylbenzidine
T zone	Test zone
WM	Whatman

ABSTRACT

In developing countries, morbidity due to infectious diseases such as diarrheal illness can cause major deterioration of physical and cognitive impairment in young children under the age of five and individuals with poor immune system. In such regions, proper diagnosis and treatment can help in changing the mortality and morbidity rates. Current tests used to detect diarrhea-causing pathogens are often expensive, time consuming, require a well-maintained centralized laboratory with continuous power supply, highly skilled laboratory personnel and good bio-safety practices, which are often limited in resource poor settings in both developed and developing countries. Real-time PCR, immunoassays (ELISA, or EIAs, lateral-flow test strips), microscopy, and flow cytometry are few examples of traditional tests available. The goal of this project was to develop a paper-based microfluidic device for detection of *Cryptosporidium* and *Giardia*, two protozoan pathogens that cause persistent to chronic diarrhea worldwide that is inexpensive and easy to use. Toward this goal, we designed and optimized a wax-printing technique to create microfluidic channels in paper that direct fluid flow via capillary action in defined patterns for colorimetric immunoassay detection of individual and multi-plexed pathogens. Initial results suggest that a minimum printed width of 300 μm was necessary to form an impermeable barrier in chromatography paper when heated at 95^{o}C for 10 min, while a minimum channel width of 1500 μm was necessary to wick fluids through the microfluidic channels. Next, we performed a concentration series of

immunolabeled *Cryptosporidium* oocysts and *Giardia* cysts to determine the lowest detectable number of oocysts in an enzyme-based colorimetric assay. Our results indicate that as few as 250 oocysts were visibly detectable for *Cryptosporidium* and 5000 cysts for *Giardia*. We further fabricated 3- dimensional (3-D) paper-based devices with a size-selective filter that excluded the use of cumbersome pre-labeling protocol to remove unbound-free antibodies by retaining enzyme-bound pathogens and measuring the amount of enzyme that reaches the bottom layer. Tests for size-selective membrane and 3-D retention assay using in-line filter holder showed that cellulose acetate membrane with 1.2 µm pore size was able to retain *Cryptosporidium* oocysts of size 4-6 µm. Follow-up assays for detection of *Cryptosporidium* in paper devices using enzyme retention assay showed potential for further improvement; however, this research provides initial proof-of-concept for paper-based microfluidic assays to detect infectious pathogens with high sensitivity using low cost materials and simple fabrication techniques.

I. INTRODUCTION

Diarrheal Illness: Background and Statistics

Globally, diarrheal disease is the 7th leading cause of death killing an estimated 1.4 million people worldwide every year, more than either malaria or tuberculosis (TB). Among these deaths, roughly half (0.751 million) are children under the age of 5 years old [1, 2]. Diarrhea can be a result of gastro-intestinal infection caused by various pathogens such as viruses, bacteria or protozoan parasites (Table 1). Diarrhea can also be exhibited as a symptom of exposure to non-infectious agents, such as environmental toxins or antibiotics. Symptoms can include watery stool, abdominal cramps, fever, bloating, vomiting, sometimes nausea, dizziness, weight loss, bloody stools and dehydration. Based upon the duration of symptoms, diarrheal illness can be classified into three major categories: (i) acute diarrhea, which is self-limiting and lasts less than 14 days; (ii) persistent diarrhea, which last between 2-4 weeks; and (iii) chronic diarrhea, which lasts more than a month [3]. Chronic and persistent cases are most often associated with severe dehydration and malabsorption leading to increased risk of death [4]. In particular, young children with nutritional deficiencies and individuals with compromised immune systems, such as HIV/AIDS, and TB patients, are at highest risk of developing persistent/chronic diarrhea that deteriorate pre-existing conditions through excessive water loss and decreased ability to adsorb vital nutrients and/or medications [5-10]. *Cryptosporidium* and *Giardia* are two protozoan pathogens that are increasingly

recognized as major causes of persistent and chronic diarrhea worldwide [3]. As such, they were selected as the initial targets for the current thesis research to develop low-cost diagnostic tests and methods for detecting diarrhea-causing pathogens.

General diagnosis and treatment

Detection and diagnosis of the etiologic agent causing diarrhea symptoms is an important factor to provide timely and appropriate treatment. Current detection methods include microscopic examination of stool, direct fluorescent-antibody tests, antigen-based tests (ELISA and lateral-flow "strip" tests) and amplification-based molecular tests (PCR) [11, 12]. These tests have analytical sensitivities ranging from 10^3 to 10^5 pathogens/g of stool with PCR being the most sensitive and acid-fast microscopy staining being the least sensitive, often requiring examination of multiple stool samples in order to confirm a negative test result [11]. With the exception of lateral-flow tests, many of the current diagnostic methods can only be performed within centralized hospital/clinical laboratories because of the high instrumentation costs and need for highly trained technicians or pathologists; therefore, access to diagnostic testing remains limited in developing countries where diarrheal illness is most prevalent.

Oral rehydration therapy (ORT) is the cornerstone of treatment for moderate to severe diarrheal illness to prevent dehydration and restore electrolyte balance bringing the bowel movements back to normal [13]. Pathogen-specific treatments are available for diarrheal illness, for instance, Nitazoxanide is an anti-protozoal agent effective against *Cryptosporidium* while Metronidazole is used to treat *Giardia* infections [11]. In addition, a range of antibiotics can be given to individuals with bacteria-related diarrhea. However, appropriate selection of these treatments requires identification of the

particular pathogen causing illness which is not routinely performed or available in developing countries, as mentioned above.

Table 1: Common diarrhea-causing bacterial, viral, and parasitic pathogens

Bacteria	Viruses	Protozoan Parasites
Escherichia coli	Rotavirus	*Entamoeba histolytica*
Salmonella	Norovirus	*Giardia lambia*
		Species / Major host: *G. lambia* – Humans; *G. muris* – Rodents; *G. agilis* – Amphibians; *G. ardeae* – Birds
Staphylococcus aureus	Adenovirus	*Cryptosporidium parvum*
		Species / Major host: *C. parvum* – Cattle, humans; *C. hominis* – Humans; *C. muris* – Rodents; *C. felis* – Cats
Vibrio cholerae		

Cryptosporidium

Cryptosporidium is a cyst forming coccidian parasite belonging to the eukaryotic phylum Apicomplexa [11]. Its infectious stage has four sporozoites that are protected by a thick-walled shell, which is resistant to normal temperatures and normal levels of chlorine that is used to disinfect water [14, 15]. These oocysts are 4 to 6 μm in diameter and typically spread to humans from bovine fecal matter in contaminated water sources and agriculture [16-18] with as few as 10 oocysts capable of causing disease [19-21]. Cryptosporidiosis, the disease caused by *Cryptosporidium* infection, is usually self-limiting in healthy individuals exhibiting symptoms like nausea, fever, abdominal pain vomiting and watery diarrhea. In high-risk populations (i.e. young or malnourished children, and immunosuppressed adults) *Cryptosporidium* infection can manifest into chronic or persistent diarrhea causing severe symptoms of malabsorption, malnutrition, growth short fall, impaired cognition or development, and even death [9, 22, 23].

Pathogen Transmission and Life Cycle

Several *Cryptospordium* species infect mammals, with *C. parvum* and *C. hominis* being the two most commonly associated with human infection (Table 1). They both are indistinguishable in terms of their morphological characteristics but they are genetically very different. *C. parvum* infects mainly ruminants and humans whereas *C. hominis* infects humans only [24]. The most common mode of transmission is the fecal-oral route through ingestion of contaminated food and drinking water, exposure at recreational water sites, or close person-to-person contact with an infected individual [16, 17, 25-27].

When infectious oocysts are ingested by a suitable host, they invade and infect the epithelial layer of the respiratory and gastrointestinal tract by excysting sporozoites [28]. In the lumen of small intestine these excysted sporozoites penetrate epithelial cells and develop into a uninucleated trophozoites within parasitophorous vacuole where they multiply asexually and develop into merozoites [28]. When these merozoites are released they invade the adjacent host epithelial cell, some cause autoinfection and the others undergo sexual multiplication forming micro-and macro-gamates [28]. When macrogamates are fertilized by microgamates, they differentiate into thin- and thick walled oocysts that are infectious [28]. Thin-walled oocysts are auto-infectious which remain in the host and are believed to cause recurring episodes of diarrhea by continuing to infect and damage microvilli causing intestines to lose its ability to absorb nutrients and water [28]. Thick-walled oocysts undergo sporogony, the process by which four sprozoites are formed, which are environmentally-resistant and infectious immediately upon excreted in formed feces [24, 29, 30]. These thick-walled oocysts are shed by an infected person with up to 10^8-10^9 oocysts released in each bowel movement, which can persist up to several months even after the symptoms have ceased [11].

Epidemiology

Many outbreaks of have been linked to inadequate disinfection of food and drinking water, or contamination of recreational water sources such as natural swimming ponds or public pools. The largest outbreak in the United States occurred in 1993 in Milwaukee, Wisconsin, when more than 400,000 people were infected with *C. parvum* due to inadequate filtration at one of the city's two water treatment plants [31]. At least 100 deaths of HIV-positive individuals were attributed to *Cryptosporidium*-related diarrheal illness during this outbreak [16]. Similarly, in 1987 in Carrollton, Georgia, 58 of 147 individuals diagnostically confirmed with *Cryptosporidium* oocysts due to treated public water supply [32].

In another instance 1984, in Tulsa, OK, stool specimens of 27/77 symptomatic children attending a day care were found to be positive for *Cryptosporidium* [33]. Stool samples from all the household contacts exposed to a child that was positive for *Cryptosporidium* demonstrated that 23% of them were positive for the presence of *Cryptosporidium* themselves, suggesting relatively high rate of person-to-person spread within individual households [33]. In 1993, an outbreak of Cryptosporidiosis was reported in Maine among students and staff who attended an agricultural fair where unpasteurized apple cider was served. When investigated, *Cryptosporidium* oocysts were identified in 160 individuals who exhibited diarrhea and vomiting. Oocysts were identified in the stool of a calf that was used to transport the apples and also on cider press, thought to be the source of infection [26].

In addition to these individual outbreaks, cumulative surveillance data from the Centers for Disease Control (CDC) from 1971-2006, indicates that there were 421,301 cases of cryptosporidiosis due to contaminated or untreated drinking water outbreaks in

the U.S. during this time period [34]. Between 2007-2008 *Cryptosporidium* was identified in 60 waterborne outbreaks and 58 of them were due to improperly treated recreational water [35]. Cryptosporidiosis surveillance reported an increase in total number of cases of cryptosporidiosis from 3505 cases in 2003 to 8269 cases in just 2005 with a slight increase of 8951 cases in 2010 [36-38]. In 2010, *Cryptosporidium* was associated with 21 outbreaks of treated recreational water causing gastroenteritis [39].

Outside of the US, *Cryptosporidium* has been identified as the causative agent in up to a quarter of all cases of diarrheal illness [11]. For instance, *Cryptosporidium* was documented to affect 444 of 1779 (25%) cases of diarrhea in children in Uganda contributing to death in some children when outcomes were tracked beyond resolution of symptoms [40]. A household survey in urban slum and rural villages of Liberia, West Africa in 1983, reported that *Cryptosporidium* was identified in 8.4% of 237 stool samples from children that presented diarrhea [41]. In a two year study conducted in Peruvian children between 1989-1991, 207 were identified with symptomatic and asymptomatic cryptosporidiosis causing short-term weight loss and, in another study, long lasting adverse effect on height in children under 5 years was seen with *C. parvum* infection [23, 42]. In Africa, a prospective survey in Kenya showed that *Cryptosporidium* prevalence was roughly 4% [43], while in Vellore, South India, a cohort study reported 53 of 452 children had cryptosporidiosis (12%) that could be traced to *C. hominis* (81%) and *C. parvum* (12%) [44, 45]. In addition to children, protozoan infections impact immune-compromised adults, such as those living with HIV/AIDS. In a study conducted in Brazil, prevalence of *Cryptosporidium* was 7% in patients with AIDS [46]. In another study, when 38 AIDS patients with asymptomatic and symptomatic diarrhea were

examined, *Cryptosporidium* was detected in 39% of the patients [47]. As demonstrated by these studies, the prevalence rate for cryptosporidiosis varies widely depending upon location, with the highest frequencies found in South America and India.

Current Diagnostic Methods

Examination of stool specimens for the presence of oocysts is the current method of choice for diagnosis in most hospitals [11]. Concentration techniques like sucrose flotation, Ritchie Formalin-ethyl acetate sedimentation combined with staining procedures like modified Ziehl-Neelson, auramine-rhodamine acid-fast staining, or direct immunofluorescence are currently most common in clinical laboratories [11]. These techniques exhibit limited sensitivity (10^5 oocysts/g stool) and sometimes generate false-positive results when fluorescent stains are used due to high background autofluorescence from stool debris or other co-infected organisms [48-51]. The spherical appearance of *Cryptosporidium* oocysts, and the presence other organisms (like yeast) in stool and stool debris often make it difficult to distinguish oocysts such that patients are frequently required to submit 2-3 stool samples for diagnostic confimation.

Immunoassays, including direct immunofluorescent assays (DIAs) and enzyme immunoassays (EIAs), that detect pathogen-specific antigens are increasingly used in health care settings and can offer improved sensitivity and specificity over traditional microscopic examinations using acid-fast staining [48, 52-54]. Routine test kits using monoclonal or polyclonal antibodies are commercially available for two-color fluorescent detection of both *Cryptosporidium* and *Giardia* with high sensitivity and specificity [55, 56]. In addition, immunochromatographic "strip" tests have been developed that offer rapid detection results with high specificity, but typically with a trade-off for sensitivity

in the detection of *Cryptosporidium* and *Giardia* [53]. For research laboratories, ELISA and molecular techniques (PCR) which are more sensitive and specific has replaced traditional microscopy [53, 57, 58]; however, these techniques are not routinely preformed in clinical settings due to the high cost of equipment and technical skill required. All of which is not readily available, particularly in resource-limited, areas due to the lack of well-established laboratories and infrastructure [59].

Giardia

Giardiasis is the gastrointestinal illness caused by a flagellated protozoan parasite called *Giardia*, which is frequently detected in humans and animals. It undergoes antigenic variation to protect itself against host's immune system causing acute and persistent diarrhea [60]. *Giardia lambia* (also known as *G. intestinalis* or *G. duodenalis*) is the most common to cause infection in both humans and domestic animals, among many species of *Giardia* (Table 1). It has a worldwide prevalence as a food-borne and water-borne pathogen causing diarrheal illness, particularly impacting developing countries lacking adequate clean water supplies [61, 62].

Pathogen Transmission and Life Cycle

Like *Cryptosporidium*, *Giardia* follows a fecal-to-oral route of transmission through contaminated drinking water, food and recreational water, or by person-person contact with poor hygiene practices. Depending on the host's immune system, the number and intensity of symptoms can vary widely from asymptomatic, showing no symptoms or changes in the host's routine when infected, to moderate/severe diarrhea, malabsorption, abdominal cramps, malnutrition, and weight loss. These symptoms can last up to several months without proper treatment and, in young children, chronic

infection has been linked to malabsorption of vital nutrients such as fat, lactose, vitamin A, vitamin B12, resulting in severe weight loss and developmental disorders [63].

The common form for *Giardia* transmission is as a cyst, an oval shaped sac approximately 7-10 μm wide and 8-10 μm long present in formed feces of an infected person or animal [61, 62, 64, 65]. Infection occurs with ingestion of just 10-25 cysts and in each bowel movement about $10^8 – 10^9$ cysts can be released [66, 67]. *Giardia* cysts are resistant to the levels of chlorine in most chlorine-treated water leaving the cysts viable and infectious when they are ingested by a host. Once *Giardia* cysts are ingested, excystation occurs in duodenum releasing trophozoites that multiply and infect the host's small intestine. Excystation is the process through which the mature *Giardia* cysts rupture its outer hard shell and releases two nucleated and flagellated trophozoites in the small intestine. The trophozoites survive the harsh conditions of the stomach and gastric acids present. The lower pH of the gastric acids may actually enhance the development of the disease. Trophozoites are 9-21 μm long and 5-15 μm wide, they attach to the mucosal layer of the small intestine using their ventral sucking disks and reproduces asexually by binary fission. They destroy intestinal epithelial brush border and block absorption of necessary nutrients and fats. The trophozoites encyst, a process in which they form cysts, travel through the colon and are ultimately released into the environment in fecal waste. The presence of bile salts and intestinal mucosa enhance trophozoite survival and encystation; although, the host-pathogen interactions and pathology of giardiasis is not completely understood [68, 69].

Epidemiology

In the United States, a total of 20,084 cases were reported in 2003, 19,140 cases in 2008 and 19,888 cases in 2010 with highest number occurring among children aged between one to nine years [70-72]. *Giardia* infects more individuals from low-income populations of US-Mexico border with 345 (81.6%) of individuals positive for *Giardia* among 77 households especially those with young children [73]. A two year study in the United States found that *Giardia* was the causative agent of diarrhea in 15% of 147 children [56].

G. intestinalis was identified as the etiological agent in 123 outbreaks caused due to drinking water in United States between 1971-2006 with 22,127 cases of giardiasis [34]. In 2003-2004, 5.6% swimming pool outbreaks were associated with *Giardia* with 766 cases of gastroenteritis caused by *Giardia* due to ingestion of treated recreational water [74]. In a study from western Nepal focused on children under 5 years of age, 35.5% of persistent diarrhea cases were attributed to protozoan infections with *G. lambia* being the most prevalent protozoan parasite (67.7%) [75]. In another study, stool samples from 164 Bedouin children in Israel, showed that the *Giardia* prevalence rate was more than 30% in young children and infants [76]. Furthermore, in a three year study between January 1999 and July 2002 following 289 Bangladeshi children with diarrheal illness for causative agents, clinical features and nutritional status, *G. lambia* was found in 11% of the stool specimens from symptomatic individuals [77]. *G. lambia* was also found in 87 stool specimens from 236 children (36.9%) who were less than 5 years of age living in the Sangkhlaburi district in Thailand when examined for intestinal parasites [78]. In Italy between 1988 and 1995, a study of Giardiasis among HIV/AIDS patients reported twenty five out of 720 (3.5%) HIV patients infected with *G. intestinalis,* of which, 22 died within

two years [79], while another study in Brazil revealed that *Giardia* was prevalent in roughly 16% of AIDS patients who had symptoms of diarrhea [46].

Current Diagnostic Methods

Similar methods are used to detect and diagnose *Giardia* infections as previously discussed for *Cryptosporidium*, with bright-field or fluorescent microscopy being the most common [56, 80]. Iodine staining or direct immunofluorescence assays, along with concentration techniques like zinc sulfate flotation or formalin-ether can be useful for the detection of *Giardia* cysts in stool samples [53, 54]. In addition, commercially available ELISA kits or rapid diagnostic tests are available for *Giardia* diagnostics which exhibit roughly 85% to 100% sensitivity and 90% to 100% specificity when compared with conventional microscopy [67, 81].

Unfortunately, the available diagnostics methods for the detection of either *Cryptosprodium* and/or *Giardia* remain expensive, time consuming, labor intensive, and require a well-established lab infrastructure or a skilled microscopist, all of which are not readily available in resource-poor settings. Therefore, there remains a need for low-cost diagnostic tools for differential detection of diarrhea-casing pathogens.

Paper-based Microfluidics: New Tools for Point-of-Care Diagnostics

Point-of-care (POC) testing has been defined by Ehrmeyer and Laessig [82] as "…a patient specimen being assayed at or near the patient, with the assumption that test results will be available instantly or in a very short time frame, to assist care-giver with immediate diagnosis and/or clinical intervention." Examples of POC testing devices available in developed countries are lateral flow or immunochromatographic test strips

for pregnancy test urine analysis, STDs like syphilis, HIV, infectious agents like *Streptococcus* and disposables with reader-like blood glucose tests [83-85].

Microfluidics is the science and technology of systems that processes small volumes of fluid within microchannels, typically ≤1000 μm in any one dimension, often formed in silicon or glass. The advantage of microfluidics is their small size which allows integration of complex laboratory tests into a miniature device. There has been a lot of development in the field of microfluidics demonstrating its advantages like manufacturing costs, fluid handling and signal detection. Microfluidics have been used in various areas such as molecular analysis, molecular biology, bio-defense and microelectronics clinical diagnostics, forensics and environmental analysis to name a few. Despite the advantages, most microfluidic-based diagnostic devices have not yet been demonstrated to be commercially successful and widely available to the end users, especially to people living in resource-limited settings [86-89].

Microfluidic POC diagnostics that are simple to use, rapid, low-cost, transportable and stable to extreme environments are highly needed that can be employed in resource-limited settings. According to the specifications suggested by World Health Organization (WHO), an ideal diagnostic test device must be ASSURED- affordable, sensitive, user-friendly, rapid, equipment-free and delivered to those in need [84]. Most microfluidics are fabricated using silica or glass which remain quite costly to make. Recently, paper-based microfluidic devices, also known as microfluidic paper-based analytical devices (μPADs), have emerged as a new class of microfluidic devices that offer several advantages over traditional microfluidics [90]. Paper is inexpensive, readily available in great quantities, it is compatible with biological samples, it is weightless, thin with

varying thickness, easy to store and transport. In addition, the white color of paper makes it a good medium for colorimetric assays and it is easily flammable so that it can be safely disposed of after use. Perhaps the most useful characteristic of paper for microfluidics is the use of capillary forces that allow fluid flow throughout the paper without the need for an external power supply or fluidic pumps [91]. Estimates for the ultimate cost, including fabrication and reagents, for paper-based microfluidic tests range from less than $0.01 to $1.00 for each µPAD [92, 93], as such, they fit well to the ASSURED criteria described above. A summary of the different paper-based microfluidic device fabrication techniques that have been reported to date is provided in the section below.

Fabrication Techniques

Photolithography

Photolithography is a patterning method that uses light and a photomask to pattern a design on a substrate, such as silicon or glass, coated with light-responsive chemicals called photoresist. This technique has been employed by the Whitesides group at Harvard to pattern microchannels in a variety of different paper types [83]. Here, the paper substrate was first soaked in photoresist and baked, then exposed to UV light after masking the paper substrate with a transparent mask that has a defined/printed pattern in black. This produced hydrophobic barriers of the photoresist that were cured by UV light (exposed to the light). When the paper substrate was washed using organic solvents, the uncured or unexposed resist washed off leaving the paper patterned with hydrophobic barriers. Drawbacks to this method stem from the use of organic solvents to remove the uncured photoresist from the hydrophilic parts of the paper causing them to become

hydrophobic, which required additional treatment with oxygen plasma to restore the paper's hydrophilicity [90, 94].

Pattern Cutting

Another method to direct fluid wicking in paper is to cut the paper in specified 2-dimensional patterns. This technique is used to prepare lateral flow diagnostic devices, the simplest type of capillary-driven devices that employ rectangular membrane strips, typically 1 cm in diameter by <10 cm in length. Instruments for paper cutting include fixed die-cutters, rotary cutters, or an x-y plotter cutter which is the most versatile. A computer controlled x-y cutting plotter has a knife in place of ink to cut sheets or rolls of paper based upon designs prepared in various computer graphics software packages. In addition, paper substrates can be embedded in between other materials, such as vinyl or adhesive tape, and cut/patterned simultaneously using a plotter cutter or other device [95].

Wax Printing or Stamping

Wax patterning is a simple and low-cost method that is used to fabricate paper-based microfluidics. It requires minimal instrumentation, such as a wax printer, wax pen, or stamp to deposit wax onto the surface of the paper [92, 93, 96]. Wax-based printing requires a computer and graphical software to design patterns that can be printed onto the paper substrate which, when heated, penetrates through the paper laterally and vertically generating hydrophobic barriers that define the interior hydrophilic channels (Figure 1). This technique generates a patterned microfluidic device and with the help of capillary forces it guides a sample to the end of a two-dimensional or three-dimensional device where embedded enzyme-based reagents can generate a colorimetric result [91, 92, 96].

Such wax-based fabrication procedures are easy and robust, with fabricated possible in less than 5 minutes, on a relatively large scale with relatively little cost other than the printer. As such, this wax patterning technique was the primary method used to generate 2-D and 3-D paper microfluidic structures in the current thesis work.

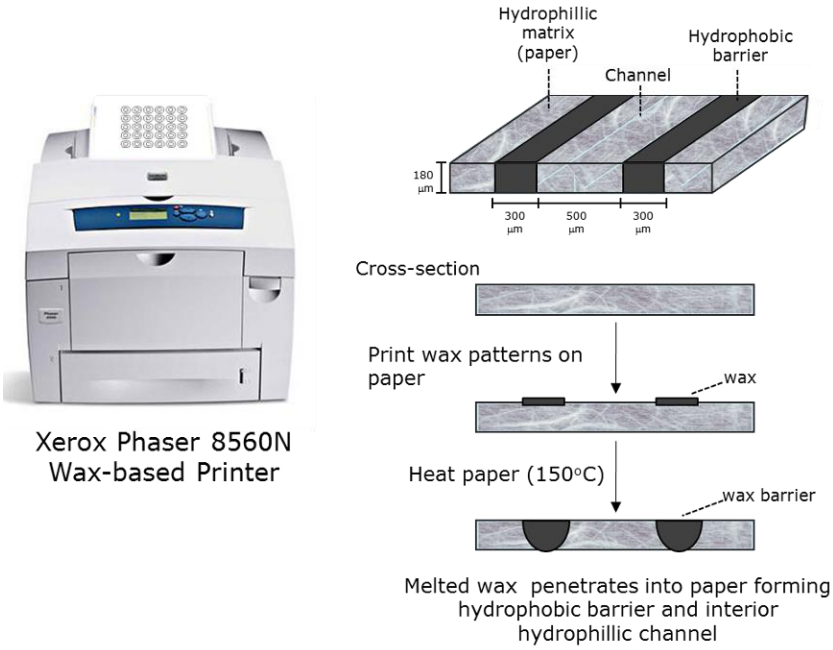

Figure 1. Schematic drawing of wax printing technique to form hydrophobic barriers that define interior hydrophilic channels for capillary-driven fluid flow.

Thesis Overview and Goals

The goal of this project was to develop a paper-based analytical device that detects the presence of diarrhea causing pathogens at the point-of-care in both developed and developing countries. As described above, diarrhea-causing pathogens are usually detected using microscopic examinations of stool, immunoassays, PCR and ELISA. Unfortunately, most of these techniques require good laboratory infrastructure, costly equipment and trained laboratory personnel, which are limited in resource-poor settings.

For such conditions, a diagnostic test that does not involve such complex procedures and expensive equipment is needed. In this thesis, two novel approaches are described that use 2-D and 3-D wax patterned paper to support simple, colorimetric assays for the detection of protozoan parasites, *Cryptosporidium* and *Giardia*. The first diagnostic approach was based upon the 2-dimentional (2-D) distribution of pre-labeled pathogens with enzyme-tagged antibodies that reacted with embedded colorimetric substrates to generate a signal visible with the naked eye. These assays were used to optimize the paper printing methods and colorimetric reactions. Next, a 3-dimentional (3-D) paper-based device consisting of folded and stacked wax-patterned papers with a size-selective barrier tailored to *Cryptosporidium* oocysts was designed and tested. Although the paper-based platform and assays still require optimization and/or re-design, knowledge gained from this work will provide valuable insight into critical parameters and design constraints for future low-cost paper-based diagnostic tests.

II. MATERIALS AND METHODS

Materials and Reagents

Whatman™ chromatography filter papers, Whatman No.1, 20x20cm square sheets (#3001-861) and No.4 24.0 cm circles (#1004-240), cellulose acetate 47 mm circles (#ST-69) and Whatman™ Syringe Type Holders, 13mm (VWR, #1980-001), used were purchased from GE healthcare (Pittsburg, PA). Double sided adhesive (3M, #5900) was purchased from Fisher Scientific (Hampton, NH). BupH Dry-Blend buffer packs were used for making Tris buffer (25mM Tris, 0.15M Nacl, pH 7.2; Thermo Fisher Scientific (Waltham, MA), (#28376) and phosphate buffered saline (PBS) (0.1M sodium phosphate, 0.15M NaCl, pH 7.2; Thermo Fisher Sci., (#28374). Each pack was mixed in 500 ml of distilled water to get 1x buffer solution. Guardian peroxidase conjugate stabilizer-diluent (Thermo Fisher Sci., #37548, proprietary formula) and Anti-*C. parvum* polyclonal antibody conjugated to HRP were purchased from Thermo Fisher Sci. (Pierce, #PA1-73185). *Giardia lambia* mouse monoclonal antibody was purchased from AbD Serotec, a Bio-Rad Company (Hercules, Cam, #MCA 2570). Conjugation of anti-*Giardia* antibody to alkaline phosphatase (AP) was performed using the LYNX Rapid Alkaline Phosphatase Antibody Conjugation Kit (AbD Serotec, #LNK012AP) according to manufacturer's instructions. Chemical substrates for colorimetric assays included nitro-blue tetrazolium and 5-bromo-4-chloro-3'-indolyphosphate (NBT/BCIP) (Pierce, #34042) and tetramethylbenzadine

(TMB) single-component mixtures (Bio-Rad, #172-1068), for AP and HRP reactions, respectively. Live pathogens of *C. parvum* and *Giardia lambia* were obtained from Waterborne Inc. (New Orleans, LA) in PBS buffer containing an antibiotic cocktail. *C. parvum* oocysts were purified from experimentally infected calves using an Iowa isolate (ref) and *Giardia lambia* cysts were from a Human isolate (H-3, aka CH-3) passaged in gerbils.

Fabrication of Paper-based Microfluidic Structures

Patterning and Printing

Microfluidic patterns and designs were created using Adobe® Illustrator® CS6 software and were printed directly onto the surface of cellulose-fiber chromatography paper using a commercially available wax printer (Xerox®, ColorQube™ 8570). The papers were heated in a toaster oven (Black&Decker® Toast-R-Oven™) at approximately 95°C for of 5 minutes or until the wax was visible from the non-printed side (i.e. bottom) of the paper.

2-D Assay Designs

Following printing and heating, 2-D assay designs were prepared by manually pipetting up to 0.8 µl of colorimetric substrate, either TMB for *Cryptosporidium* (2x) or NBT/BCIP for *Giardia* (3x), into the outer reaction zones. Devices were allowed to air dry at room temperature for at least 5 minutes. During an assay, paper devices were suspended between two microfuge tub racks to prevent uneven wetting or absorption of reagents/pathogens onto bench paper.

3-D Assay Design and Assembly

Single pathway 3-D design

The single pathway 3-D device consisted of two layered wax patterned paper with a single inlet for sample addition that follows a vertical fluidic path to the next layer. This design has a single reaction zone that was pre-spotted with 0.8 μl- 2x TMB or 3x NBT/BCIP. A smaller pore size filter material, like cellulose acetate with 1.2 μm pore size, was hole punched using a ¼" McGill punch and was embedded between the two layers using double-sided adhesive. At the time of the assay binder clips were used to hold the device together to ensure close contact between the layers.

Dual pathway 3-D design

The 3-D layered device shown in Figure 1 was a multilayered, accordion folded series of wax-patterned papers that had a cellulose acetate filter (pore size 1.2 μm) embedded between two of the layers. Each individual layer of the 3-D device consisted of a wax patterned 2-D sheet. Before folding, the bottom layer was spotted and dried with 0.8 μl single-component TMB colorimetric substrate at the visible reaction zones denoted control, C and test, T. Then each individual wax pattern was folded between each other at appropriate places to achieve a layered structure. A cellulose acetate filter was then embedded between layers 3 and 4 using double sided adhesive. All layers were then enclosed in a glossy laminate that had a single exposed inlet for addition of sample at the top sample loading zone. Two medium and two small binder clips were used to ensure close contact between each layer during the assay. Within 15 min of sample addition, the reaction zones, the C and T were visually inspected and then scanned for quantitation purposes as described below.

Pathogen Immunolabeling

With Centrifugation to Remove Un-bound Antibodies

For 2-D and 3-D assays, 1x 10^6 total organisms in 0.1% PBSA or Guardian buffer (GB) were incubated with 200 – 400 µg/mL of anti-Crypto/HRP antibody (1:5 dilution from stock Ab solution in 50 µl total volume), or 100 µg/mL of anti-Giardia/AP antibody in 0.1% TBSA (1:10 dilution from stock Ab solution in 100 µl total volume) for 1 hr. at room temperature, protected from light. Following incubation, the samples were washed three times in 0.1% PBSA, GB or in 0.1% TBSA by centrifugation at 2000xg for 10 minutes. The immunolabeled pathogens were stored at 4ºC for up to one week. This method is sometimes referred as "pre-labeled prewashed" within the remaining thesis text.

Without Centrifugation for Direct Assay in 3-D Paper Structures

The 3-D *Cryptosporidium* enzyme retention assay approach described in Figure 2 did not require the removal of unbound antibodies from the immunolabeled pathogens. Here, 5 x 10^3 - 1 x 10^5 oocysts were incubated with a dilute anti-Crypto/HRP antibody solution (100 – 800 ng/mL) in 15 µl - 400 µl of 0.1% PBSA or GB for 1 hr. at room temperature, protected from light. This solution containing pathogen-bound antibodies and unbound antibodies (sometimes referred as "pre-labeled unwashed") was added directly to the sample zone of a 3-D device or in-line filter holder containing size-selective membranes.

Measurement of Signal Intensity, Plots and Statistical Analysis

Three different methods were used to measure the colorimetric signal intensity depending on the type of assay performed; (i) visual inspection of the paper devices, (ii)

ImageJ quantification of digitally scanned devices, and (iii) UV/Vis absorbance for in-line filter tests. Visual inspection of colorimetric assays was a simple and easy technique that eliminated the need of expensive optical equipment, but for long-term digital storage and analytical purposes, the colorimetric signal of the devices was digitized using a flatbed scanner (EPSON, #V500) and analyzed using ImageJ [97] open-source software. An example of the ImageJ analysis sequence used for the paper-based immunoassays is shown in Figure 2. Here, the scanned RGB images were separated into their red, green, and blue color channels. The images were inverted and the grey-scale intensities from the red-channel was used with three different region of interest (ROIs) of same area size (0.114 cm^2) were chosen to measure the signal intensity in one reaction zone. The average of these three ROIs were then plotted on a concentration vs grey intensity graphs using ∑SigmaPlot™ (© Systat Software Inc., San Jose, California). To the plotted data, curves were fit using standard four parameter logistic curve. After curve fitting, both the analytical limit of detection (LOD) and limit of quantitation (LOQ) values were calculated and plotted on the graphs. The LOD is the lowest quantity of a substance that can be detected above the blank, which was designated as three standard deviation above the zero concentration control (0±3SD). LOQ is the signal of a particular substance which can be distinguished from its consecutive signal vales, which is calculated as ten standard deviations above zero concentration control (0±10SD).

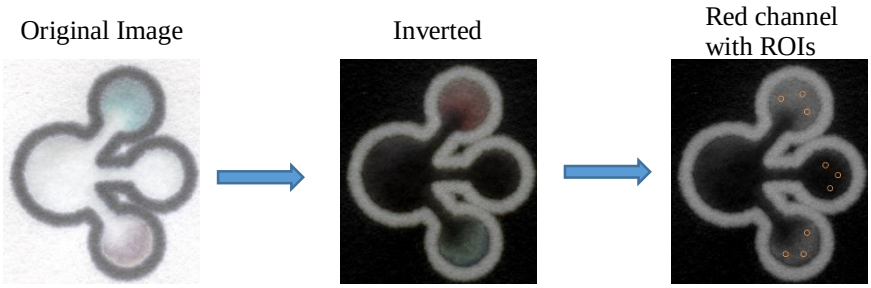

Figure 2: Measurement of colorimetric paper-based signal intensities using ImageJ. Original image of a multi-plex assay was scanned and then inverted in ImageJ from drop menu. This was then split into red, blue and green channels by selecting split channels. Circular tool was selected to make ROIs (represented here in small orange circles) that measures the signal intensity of the area selected.

In-line Filter Tests

Size-selective membrane characterization

Triplicate samples of *Cryptosporidium* (50,000 oocysts in 1 ml PBSA) immunolabeled according to the methods described above with centrifugation, were passed through cellulose acetate, poly-track etched carbonate or Whatman chromatography No.1 filter materials inside a 13 mm in-line filter housing using a syringe pump at 200 µl/min flow rate. Syringe, inline filter holder and the tubing were washed between each sample by flushing PBSA buffer (3x 1000 µl) and parts of the filter holder were also sonicated in a water bath between runs. Flow through from each sample (200 µl) was incubated with TMB substrate (100 µl) for 20 minutes and the absorbance intensity at 655nm was measured in a 96-well microplate (Synergy™ H1 Hybrid multi-Mode microplate reader, BioTek, Winooski,VT). In addition, a portion of the flow through was centrifuged at 2000xg for 5 min. The supernatant was discarded and any oocysts were resuspended for counting in a hemacytometer. Positive control did not

contain an embedded filter membrane such that 100% of the oocysts were expected to pass through the holder.

Non-specific binding interactions

An HRP-antibody solution (anti-crypto tagged HRP at 800 ng/ml) was prepared in 0.1% PBSA, 0.1% PBSA with 0.05% triton-X or 0.1% PBSA with 0.05% tween-20, then passed through cellulose acetate filter membrane in 3x replicates. Absorbance at 655 nm was measured in 200 µl of flow through reacted with 100 µl TMB reagent as described above. Buffers with same antibody concentration were added directly to the microplate as a positive control for this experiment.

Cryptosporidium enzyme depletion proof-of-concept

A series of *Cryptosporidium* oocyst samples containing 0 to 100,000 oocysts were pre-labeled with 160 - 800 ng/ml antibody according to the pathogen immunolabeling without centrifugation protocol described above. Each series was performed in duplicate or triplicate, passed through an in-line filter holder with a 1.2 µm cellulose acetate membrane and stored at RT or 4˚C prior to analysis.

Stability study for HRP

Antibody concentration of 800 ng/ml was spiked into buffers 0.1% PBSA and Guardian buffer (in 2x replicates), one replicate stored at RT and the other on ice. From 0hrs to 3hrs at every 30 minute interval, 100 µl of each sample was incubated with TMB in a 96 well microplate and read for its absorbance as described above.

III. RESULTS

Characterization of Wax Printed Hydrophobic Barriers in Various Cellulose Paper Materials

The formation of hydrophobic wax barriers in paper using the Xerox ColorCube 8570 wax printing technique described above requires that the wax, when melted, penetrates through the full thickness of the paper. The melting process results in both vertical and horizontal spreading of wax from the surface. Thus, the amount of wax needed to form a solid hydrophobic barrier varies based upon the physical properties of the paper substrate, including the thickness and porosity (i.e. density of the fibers), and must be characterized for each paper type used in a paper-based microfluidic device. In order to identify the minimum line width needed to form a solid hydrophobic barrier in Whatman No. 1 and No. 4 chromatography paper, a series of straight lines with different widths that ranged from 50 μm to 300 μm were printed and heated then tested for their ability to prevent a dye solution from crossing the barrier (Figure 3).

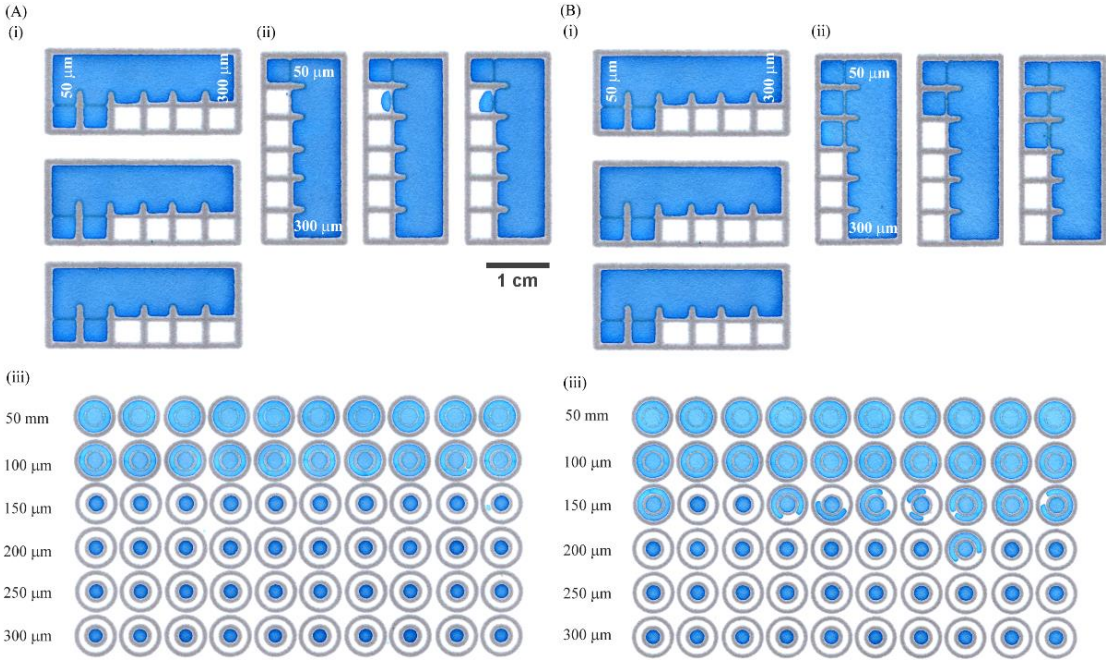

Figure 3. Comparative assessment of wax-printed hydrophobic barriers in different paper materials. Whatman chromatography No.1 (A) and Whatman chromatography No.4 (B) was designs were prepared to determine the minimum printed width of a line needed in order to establish hydrophobic barrier. Panels (i) were printed with horizontal lines in three replicates, panels (ii) were printed with vertical lines in three replicates and panel (iii) were printed in radial designs in ten replicates. Barrier widths ranged from 50 µm to 300 µm at 50 µm intervals. Lines printed on Whatman chromatography No. 1 yielded better barriers in vertical and circular resolutions.

In Whatman No. 1 chromatography paper, with a pore size of 11 μm and a thickness of 180 μm, a minimum printed horizontal and vertical line width of 150 μm was needed to form a solid hydrophobic barrier (Figure 3A, i and ii). A test of the combined horizontal and vertical printing width was also examined in a radial design with 100% barrier failure occurring when printed at 50 μm and 100 μm thickness, 10% failure occurred when wax was printed at 150 μm thickness, and 0% failure when printed at ≥200 μm thickness (Figure 3A, iii). Slightly greater line widths were needed for formation of wax barriers in Whatman No 4. paper which possessed a larger pore size of 25 μm and an equivalent thickness of 180 μm (Figure 3B). In this material, the minimum printed horizontal and vertical line width was 200 μm (Figure 3B, i and ii), while the minimum radial line width was 250 μm (Figure 3A, iii). To be conservative, a 300 μm printed width was established as the minimum line width for all subsequent paper-based microfluidic designs using these paper materials.

When heated, a 300 μm printed wax line spread to over four times its original size (1,290 ± 13.4 μm) based upon 10 measurements along a straight line (data not shown). Since two parallel wax barriers were needed for the formation of a hydrophilic channel that could then define the path of fluid flow through the paper, the minimum separation distance between wax printed lines was also examined. As shown in Figure 4, out of eight different channel widths ranging from 1 mm to 2 mm, a minimum of 1.5 mm between printed lines (pre-heated distance) was required in order to wick fluids through a 2.4 mm long wax-formed channel. The average width of this channel was 587 ± 25 μm after heating. A width of 1.4 mm was sufficient to wick the dye into the channel; however, there was noticeable lack of uniformity within the channel that could adversely

affect flow (Figure 4, arrow). Thus, a minimum channel width of 1.5 mm was used for all subsequent paper-based microfluidic designs.

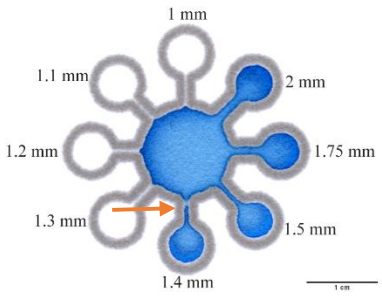

Figure 4. Minimum printed channel width for capillary-driven fluid flow. A 2-D device with constant circular zones and varying parallel line widths ranging from 1 mm to 2 mm was prepared in Whatman No. 1 cellulose paper. When a dyed buffer was added to the center of the device, the solution was wicked to the circular zones by capillary forces.

2-Dimensional Paper-based Microfluidic Assays

Colorimetric assay for detection of C. parvum oocysts

To establish a proof-of-concept for paper-based immunoasssays, a wax-patterned device with constant channels and reaction zones was used to detect the presence of *Cryptosporidium* by development of a colorimetric signal and also determine the appropriate amount of substrate. The wax-patterned devices shown in Figure 6 have a central sample loading zone, eight hydrophilic channels and eight test zones embedded with varying volumes of TMB substrate. The negative control and device containing 4,000 pathogens showed no visible enzyme signal development, while a visible blue color was apparent in devices with 40,000 oocysts and 400,000 oocysts (Figure 5). Assuming that there was a uniform distribution of oocysts throughout the device in the sample zone, channels, and all reaction zones, the minimum number of oocysts needed to

elicit a visible reaction was less than 2,500 based upon the area fraction of a single reaction zone (6%). A progressive increase in color intensity was also seen with an increase in the amount of substrate ultimately reaching saturation at 0.8 μL of TMB deposited (Figure 5, clockwise reaction zones). Since it was the enzyme-bound pathogen and not the substrate that should be the limiting factor of the assay, all future experiments were performed with a minimum of 0.8 μl of reagent embedded within the reaction zone.

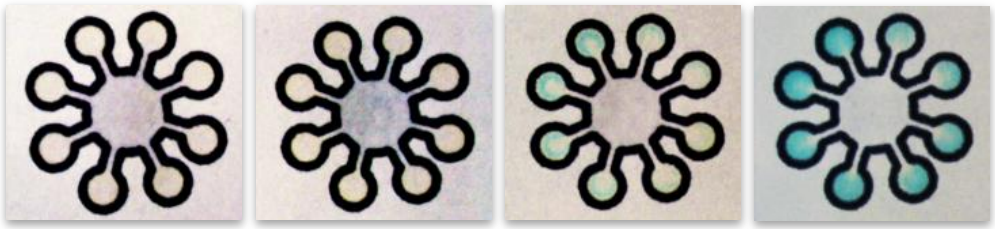

Figure 5. 2-D *C. parvum*-tagged HRP colorimetric assay with increasing numbers of oocysts. A visible signal appeared with as few as 10^4 oocysts and increased directly with the number of oocysts and substrate volume (clockwise in duplicate 0.2, 0.4, 0.6 and 0.8 μl).

Multi-plex Assay for Detection of C. parvum and G. lambia

Theoretically, each reaction zone in the 2-D paper microfluidic structures above could be used to detect distinct pathogens. To test this hypothesis, HRP-immunolabeled *Cryptosporidium* and AP-immunolabeled *Giardia* were examined in a series of multi-plexed 2-D assays with increasing numbers of cysts/oocysts. Scanned images of assays containing 0 – 25,000 *Cryptosporidium* and *Giardia* pathogens are shown in Figure 6A. Based upon visible inspection, a blue HRP colorimetric signal became apparent in assays with as few as 250 *C. parvum* oocysts while the purple-ish alkaline phosphatase color became evident above 5,000 Giardia cysts. A plot of the signal intensity generated by

each pathogen versus concentration is shown in Figure 6B and C on both linear and logarithmic x-axes, panels i and ii respectively. Linear plots showed a rapid increase in signal intensity followed by a gradual decrease in signal intensity after reaching saturation with increasing number of enzyme-bound pathogens. Using a 4-parameter logistic curve fit, the analytical limit of detection (LOD), for *Cryptosporidium* was found to be at 163 oocysts and 3,152 for *Giardia* cysts. Limit of quantitation (LOQ) is at 461 for *Cryptosporidium* (Figure 6B-i and C-i). LOQ was not determined for *Giardia* because of the large standard deviations found in the controls.

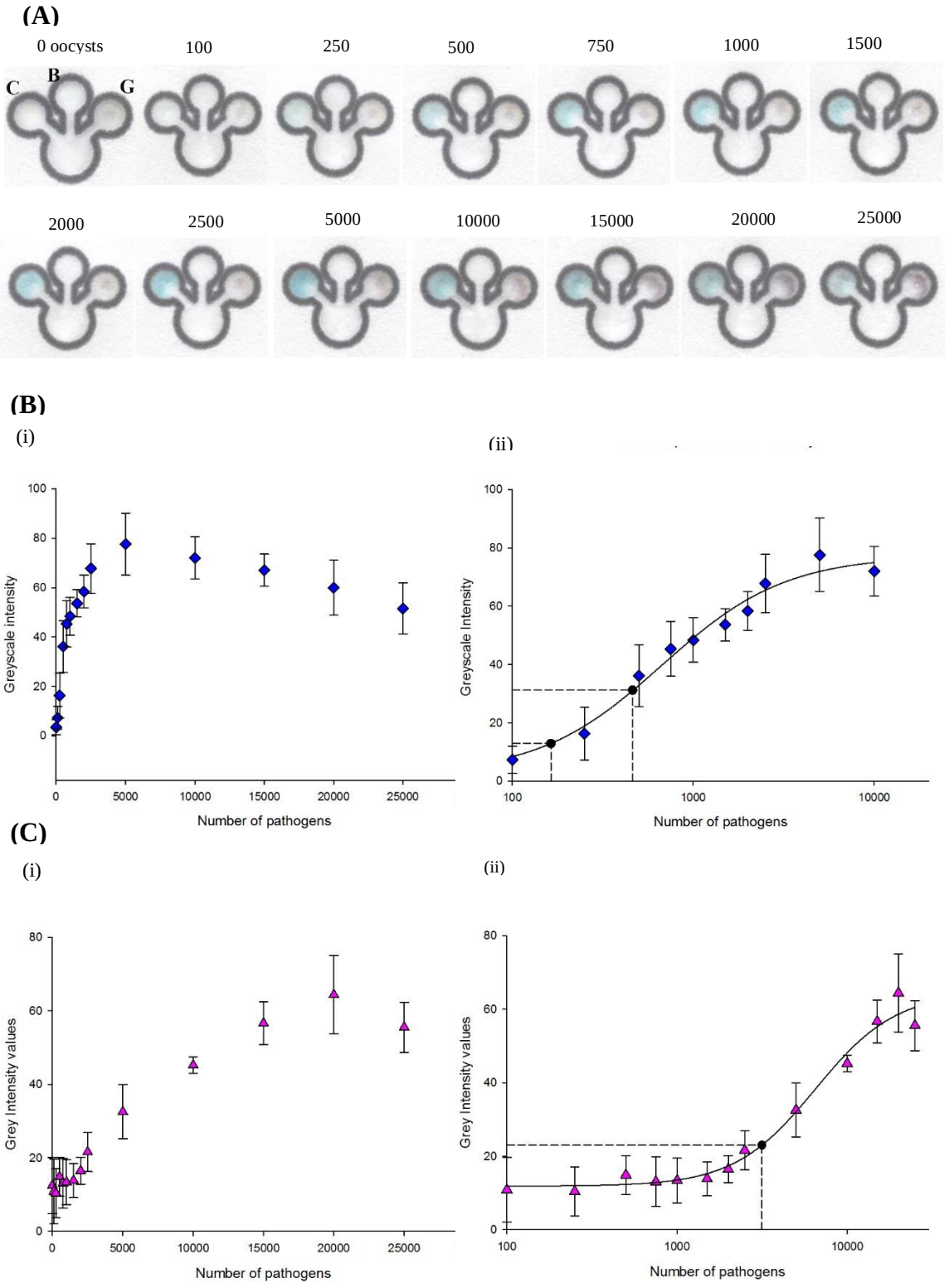

Figure 6. Multi-plex 2-D colorimetric assay for *Cryptosporidium* and *Giardia*. (A) Scanned images of the paper-based devices following HRP and AP enzyme development were used to quantitate signal from (B) *Cryptopsoridium* and (C) *Giardia.* Normalized intensities were plotted in linear and on log plot (B, panels i, ii and C, panels i, ii respectively). Black circular dots on curves represent LOD and LOQ.

3-Dimensional Paper-based Microfluidic Assays

For the detection of *Cryptosporidium* and *Giardia* in 2-D colorimetric assays described above, pre-labeling of cysts/oocysts was required that involved washing off unbound antibodies. To eliminate the need for centrifugation in this labeling and washing process, a 3-D paper-microfluidic approach was devised to measure antibody-HRP enzyme depletion in the presence of *Cryptosporidium* oocysts by size selective retention on a filter membrane. This multi-layered device contained a single inlet for sample loading that then distributed the sample to a control and test zone in two separate vertical pathways. A size-selective filter that could retain one or more of the pathogens, *C. parvum* or *G. lambia*, was embedded within the layers of the device along the test pathway as shown in Figure 7. In theory, when a *C. parvum* oocyst sample incubated in solution with the enzyme-tagged antibodies are added to the device, the unobstructed path that leads to control zone would allow both pathogen-bound and unbound antibodies to reach the bottom layer of the device where colorimetric substrates are embedded, whereas the path that leads to test zone containing a size-selective filter would retain any oocysts present along with their bound antibodies/enzymes. Thus, the test pathway depletes the overall amount of enzyme reaching the reaction zone. The presence of oocyst pathogens would be expected to reduce the colorimetric signal in the test zone compared to the control zone in this 3-D "enzyme depletion" assay approach.

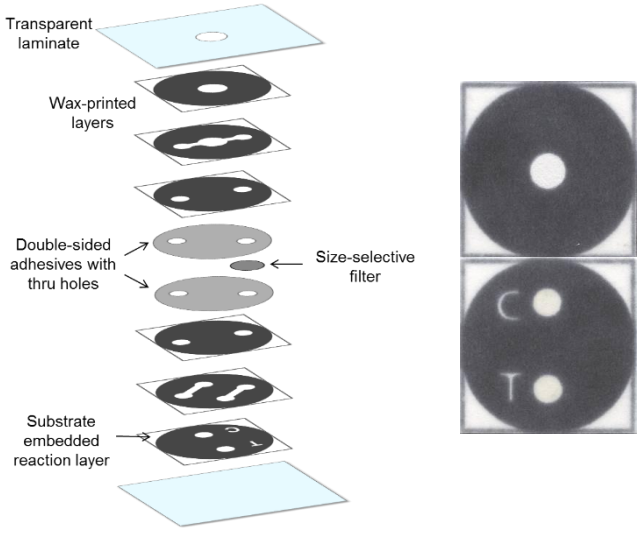

Figure 7. 3-dimentional paper-based device for *Cryptosporidium* enzyme retention assays. Each layer is a 2-D device that is layered on top of each other and sealed by a transparent laminate that has an opening at the inlet or sample loading zone. A size-selective layer is embedded (between double-sided adhesive) with in the path that leads to test (T) zone. To the right is top and bottom view of a fully assembled 3D device

Size-Selective Membrane Characterization

A series of experiments, summarized in Table 2, were performed using an in-line filter holder to determine a suitable size-selective filter membrane that could retain pathogens such as *Cryptosporidium*, with an average oocyst size of 4-6 µm. The positive control (no membrane or filter) had highest A_{655} TMB color development, indicative of the presence of pre-labeled/pre-washed HRP-antibody tagged oocysts in the flow through. Of the membrane materials, the polycarbonate membrane passed the largest number of oocysts (150 x 10^4/ml) and exhibited the highest enzymatic activity in the flow through (1.26 ± 0.00) (Table 2). The cellulose acetate filter membrane with a 1.2 µm pore size showed zero or no oocysts present in its flow thorough but there was some non-specific enzymatic activity generating a signal intensity of 0.332 ± 0.11 above the blank PBS control (Table 2). Based upon these results, only the cellulose acetate membrane was deemed to be a suitable membrane/filter material capable of retaining enzyme-bound *Cryptosporidium* pathogens in subsequent 3-D paper-based assays.

Table 2: Filter membrane efficiency for *Cryptosporidium* retention

Paper/Filter Material	Nominal Pore Size (µm)	Absorbance values at 655nm	Number of cells* present in flow-through (10^4/mL)
No filter (control)	--	1.45 ± 0.01	347
Cellulose Acetate	1.2	0.33 ± 0.01	0
Polycarbonate	5.0	1.26 ± 0.00	150
Whatman No.1	11.0	0.97 ± 0.03	28

***** Cell counts determined using a hemacytometer are only estimates due to the presence of large clusters

Single Pathway 3-D Enzyme Retention Assay

Whatman No. 1 cellulose paper was wax printed and layered/folded to form a 3-D device with a single vertical fluid pathway as shown in Figure 8. A cellulose acetate

membrane was embedded between two of the layers (shown in orange, Figure 8A) using cut double-sided adhesive, such that any HRP-antibody bound Crypto oocysts with a sample flowing through the device would get retained allowing the remaining unbound HRP-antibodies to flow vertically through to the colorimetric reaction zone on the bottom paper containing TMB substrate. A matrix of different antibody concentrations were tested at high/low pathogen levels and compared to a negative control (Figure 9). A slight decrease in color intensity was apparent upon visual inspection between 0 oocyst controls and those containing 50-100 thousand oocysts, particularly at an antibody concentration of 200 ng/ml (Figure 9). When quantified, the HRP signal intensity decreased at least 30% in the presence of 50-100 thousand oocysts relative to the controls at an antibody concentration of 200 ng/ml (Table 3, highlighted in blue). However, this trend did not hold true for all antibody concentrations or with increasing pathogen numbers (Table 3). In addition, there was a relatively large amount of variation in color intensity, even among controls, such that the 800 ng/ml control exhibited less color development than the 400 ng/ml control (Figure 9), suggestive of enzyme saturation/inhibition at high antibody concentrations. Therefore, 200 ng/ml HRP-antibody was used in all further enzyme retention experiments.

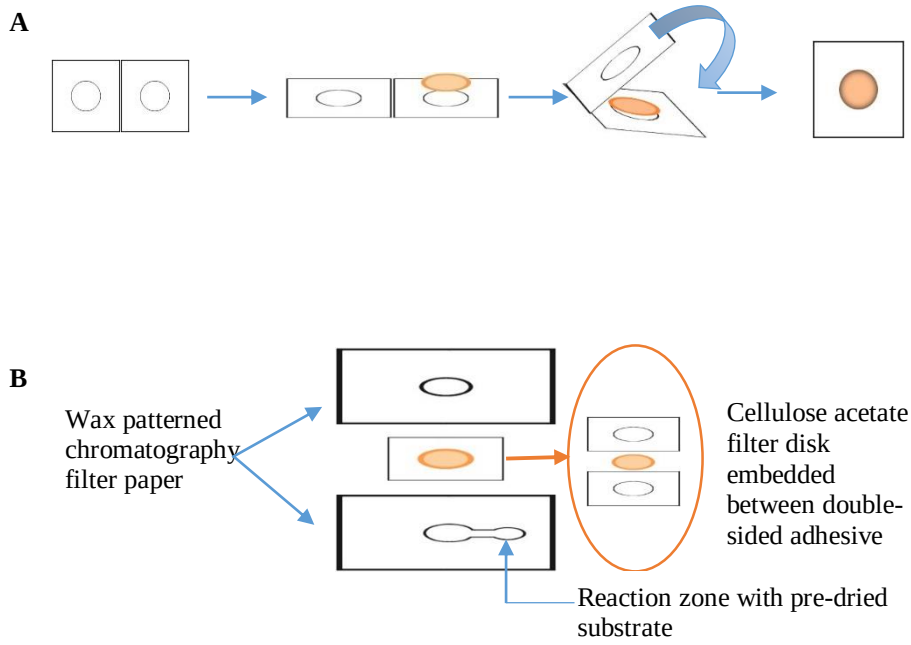

Figure 8. Fabrication of Single pathway 3-D device. Cellulose acetate membranes were sandwiched between two circular cut double-sided adhesives (A) then embedded between two layers of 2-D wax-patterned Whatman No. 1 papers spotted with TMB colorimetric substrate.

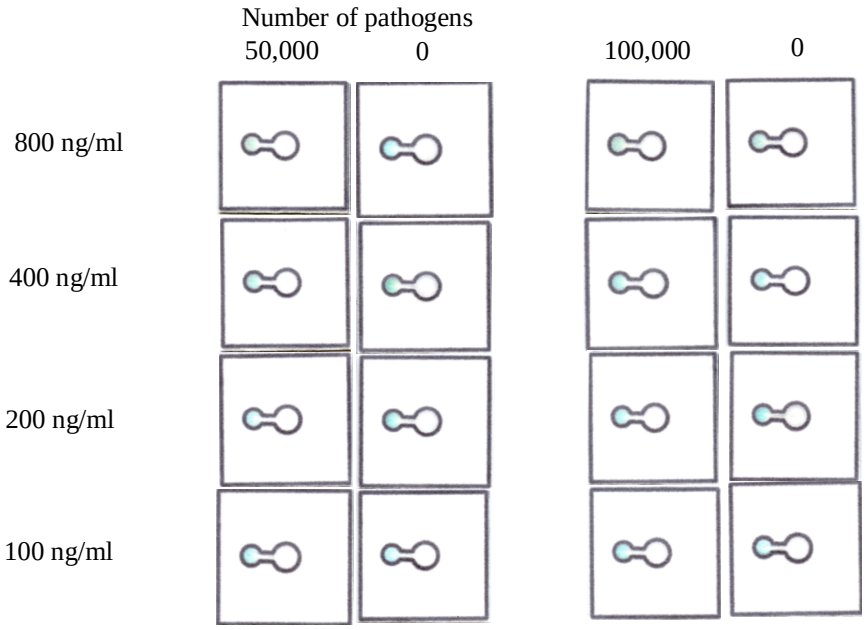

Figure 9. Single pathway 3-D enzyme retention assay at varying antibody concentrations. Each sample was compared against its control with equal antibody but 0 oocysts.

Table 3: Quantified results of single pathway 3-D enzyme retention assay

Antibody concentration	50,000 oocysts	Control	100,000 oocysts	Control
800 ng/ml	40.9 ± 4.9	55.8 ± 7.5	55.2 ± 5	51.6 ± 8.9
400 ng/ml	53.7 ± 6.6	79.8 ± 8.1	60.2 ± 8.5	55.8 ± 3.2
200 ng/ml	42.9 ± 6.4	70 ± 13.4	53.9 ± 4.9	77.2 ± 11.5
100 ng/ml	52.8 ± 12.1	44.4 ± 5	54.9 ± 3.3	40.5 ± 4

Dual Pathway 3-D Enzyme Retention Assay

The dual pathway 3-D paper microfluidic design described in Figure 7 aimed to eliminate some of the variation seen in the single-pathway devices by incorporating an internal assay control into the test structure. In this device one pathway (test pathway) was obstructed with the cellulose acetate size-selective membrane and the other remained unobstructed (control pathway), both the control and test pathways dead ended on TMB

reaction zones. In the initial experiments, pre-labeled unwashed *Cryptosporidium* samples (containing 0 oocyst and 50,000 oocysts, respectively) were added to the inlet of the dual pathway 3-D device and allowed to react. A similar intensity of color/reaction development was found in each control (C) and test (T) zone regardless of the presence or absence of pathogen (Figure 10).

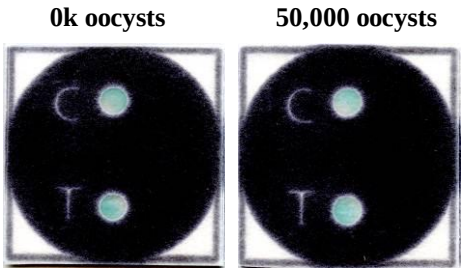

Figure 10. Dual pathway 3-D assay performed using HRP-immunolabeled oocysts that has unbound antibodies that are not washed off. Negative control (0k) has no oocysts therefore an equivalent color development was expected whereas the device with 50,000 oocysts was expected to develop a lower signal in test zone compared to its control zone.

With the presence of size-selective filter membrane, only unbound antibodies were expected to reach the test zone developing a blue color that is less intense than color development in control zone. Therefore, a follow-up 3-D assay was performed using a pre-labeled pre-washed oocyst samples. Devices with 0 oocysts, 1000 oocyst and 5000 oocysts showed no color development in any zones but colorimetric signal was apparent in 10,000 and 50,000 oocyst sample devices with increase in signal from low to high concentration of oocysts (Figure 11). There was no difference in color observed between

the C and T zones of 10,000 and 50,000 oocyst sample devices (Figure 11).

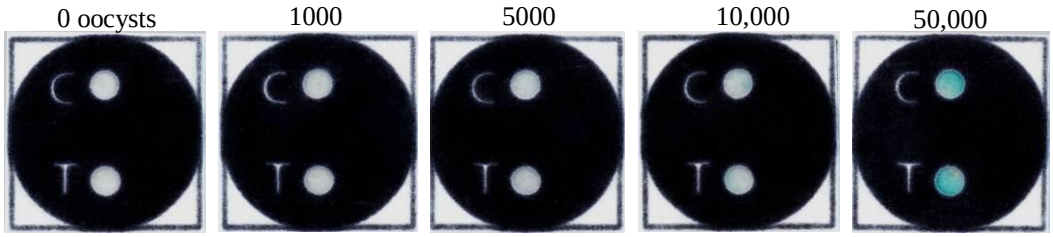

Figure 11. Dual pathway 3-D HRP enzyme assay using pre-labeled and pre-washed samples containing increasing numbers of *Cyptosporidium* oocysts. Colorimetric signal was apparent at higher concentrations but test zones were not expected to turn blue in this enzyme retention assay.

Since there were little/no unbound antibodies expected in the sample due to pre-washing, a strong difference in signal intensity was anticipated between the control (positive/blue) and test zones (negative/white) due to the presence of cellulose acetate filter membrane in its pathway blocking any HRP-bound oocysts from reaching the TMB substrate. The results presented in Figure 11 clearly did not fit this model. Several potential sources of this unexpected non-specific reaction were examined in further detail in order to troubleshoot the assay methodology, design and/or approach.

Non-specific Interactions of Antibody to Filter Material

In order to determine the cause of non-specific signal seen in the above dual pathway 3-D enzyme retention assays in paper-based devices, a series of in-line filter tests were performed to examine non-specific enzymatic interactions of various paper/filter materials, used in fabricating a paper device, in different buffer compositions. Figure 12 shows the percent recovery of an HRP-antibody solution when passed through each filter. Samples passed through cellulose acetate had better recovery of antibody when surfactants were added to PBSA buffer, almost 100%, than PBSA only with 74%. Whatman No.1 was another material used in fabrication which was also examined along with polycarbonate. Buffer with tween-20 was seen to yield better recovery of antibody

than others (Figure 12). High percentage recovery of more than a 100% with Whatman filter material could be due to the presence of residual paper impurities and also paper debris in the flow through when sample was purged through the filter holder.

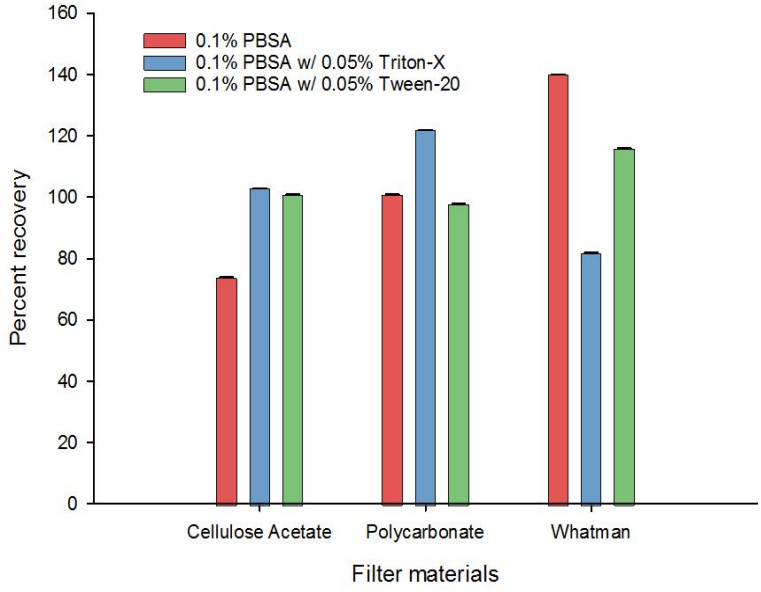

Figure 12. Measurement of recovery of antibody passed through different filter materials. With 0.1% PBSA, large variations in percent recovery was seen in all materials. Addition of tween-20 reduced the non-specific enzyme activity seen when other buffers used. Controls were directly read for absorbance at 655 nm.

As told by a Whatman representative, the WM chromatography No.1 filter paper was not treated or processed using hydrogen peroxide. With the addition of 0.05% tween-20 in 0.1% PBSA, both excess and loss in recovery of antibody was normalized close to a 100% recovery in both cellulose acetate and WM filters. Next step was to determine if the samples were flowing around the filter embedded between double-sided adhesive in dual pathway 3-D retention assays. Therefore, an enzyme retention assay was performed using inline filter holder that excludes the use of double-sided adhesive and Whatman No.1 chromatography paper material.

Enzyme Retention Assay Proof-of-concept using Inline Filter Holder

A series of *Cryptosporidium* oocyst concentration was passed through inline filter holder. To use inline filter holder a larger sample volume was needed than paper-based microfluidic devices therefore an antibody concentration series was performed to get direct absorbance for the anti-Crypto-HRP antibody. Known antibody concentrations were prepared, 2000 ng/ml to 200 ng/ml in 100 ml PBSA buffer, was incubated with TMB and read for absorbance (see methods for measurement of signal intensity). The absorbance for each concentration of antibody is shown in Table 4.

Table 4: Antibody concentration series using 96-well plate

Antibody concentration	Mean absorbance(3x A_{655})
CTRL	0±0.003
2000 ng/ml	1.63±0.059
800 ng/ml	0.70±0.041
400 ng/ml	0.35±0.033
200 ng/ml	0.17±0.028

A *Cryptosporidium* concentration series incubated with 800 ng/ml antibody in 0.05% Tween-20 in 0.1% PBSA buffer (using more than 800 ng/ml may cause saturation or inhibition of the enzyme) was passed through In-line filter. Absorbance intensities to pathogen concentration are plotted in Figure 13. There is an increase in absorbance intensities of each sample increased with increasing number of oocyst in that sample. The sample with 100,000 oocysts had 0.061 absorbance and the sample with 0 oocyst had absorbance intensity of 0.016 (Figure 13). It was anticipated that with the presence of cellulose acetate and oocysts, the amount of unbound enzyme reaching the reaction would decrease with increase in oocyst concentration. The outcome of this assay was

unexplainable at this point which does not help to prove the failure or success of the 3-D retention assay in paper-based devices. However there was loss of enzyme activity observed from 0.7 of 800 ng/ml antibody conc. in Table 3 to 0.1 in the above assay. This loss of enzyme activity was studied for HRP at RT and on ice.

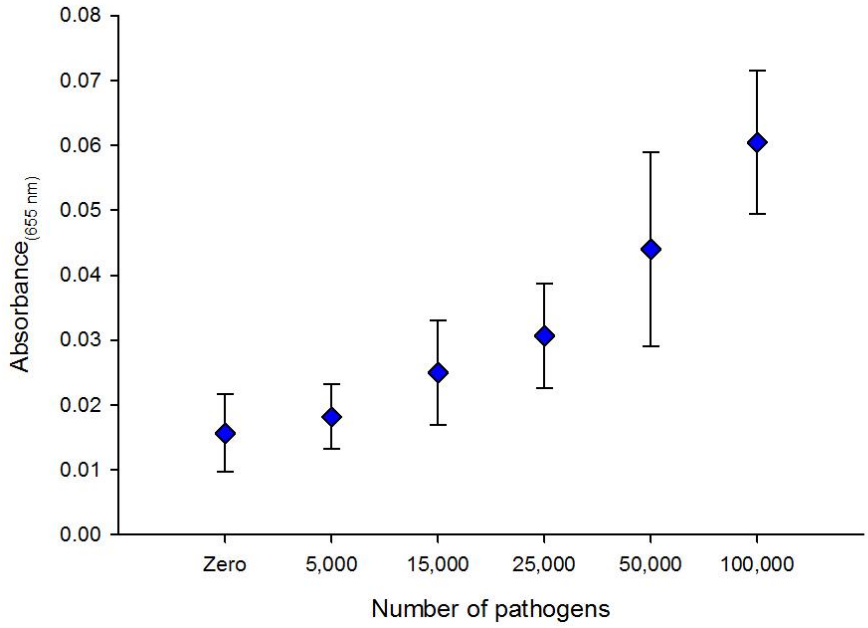

Figure 13. *Cryptosporidium* concentration series in PBSA using in-line filter enzyme retention assay. Concentration series of Cryptosporidium (0, 5000, 15000, 25000, 50000 and 100000 oocysts) in 0.1% PBSA with 0.05% tween-20. Absorbance intensities are graphed against concentration of oocysts. The intensities increase with the concentration of oocyst.

Examination of Horseradish Peroxidase Enzyme Stability

The enzyme horseradish peroxidase conjugated to the antibody develops a visible blue color in the presence of TMB substrate by oxidizing it. Suggested storage temperature of the enzyme conjugated antibody was at 4ºC but during immunolabeling incubation period and in-line filter assays samples were all stored at RT from a minimum of 1 hour to about 4 hrs (hours). Protein degradation was likely possible in such

conditions that could affect the colorimetric signal of these enzymatic assays. So a stability study was conducted for HRP tagged antibody at 800 ng/ml antibody concentration (Table 5, Figure 14).

Within the first 30 minutes, more than 75% loss of enzyme activity was observed at RT and about 97% loss in 3 hrs (Table 5, Figure 14). Even when stored on ice, there was more than 70% of loss of enzyme activity in 3 hrs. Therefore, an experiment that took more than 3 hrs likely had no or very little enzyme activity remaining (as in the above enzyme retention assay).

A HRP stabilizer like Guardian Peroxidase Conjugate stabilizer-diluent (Guardian buffer) helps to maintain the activity of the enzyme at dilute and different storage conditions. The stability of the enzyme was tested similarly to the above (Table 5, Figure 14). HRP in stabilizer seemed to have little or no loss of activity even at 3 hrs of storage at RT making it a better diluent buffer to work with in further assays

Table 5. HRP enzyme stability study in PBSA and GB

Time	PBSA at RT	PBSA on ICE	STABILIZER at RT	STABILIZER on ICE
0 min	0.722±0.03	0.672±0.03	0.50±0.02	0.45±0.02
30 min	0.158±0.004	0.511±0.02	0.47±0.04	0.46±0.03
60 min	0.077±0.004	0.346±0.01	0.51±0.01	0.47±0.05
90 min	0.054±0.01	0.277±0.01	0.55±0.01	0.53±0.01
120 min	0.040±0.001	0.219±0.02	0.70±0.13	0.56±0.07
150 min	0.029±0.000	0.174±0.02	0.52±0.04	0.50±0.01
180 min	0.021±0.001	0.144±0.004	0.54±0.05	0.50±0.01

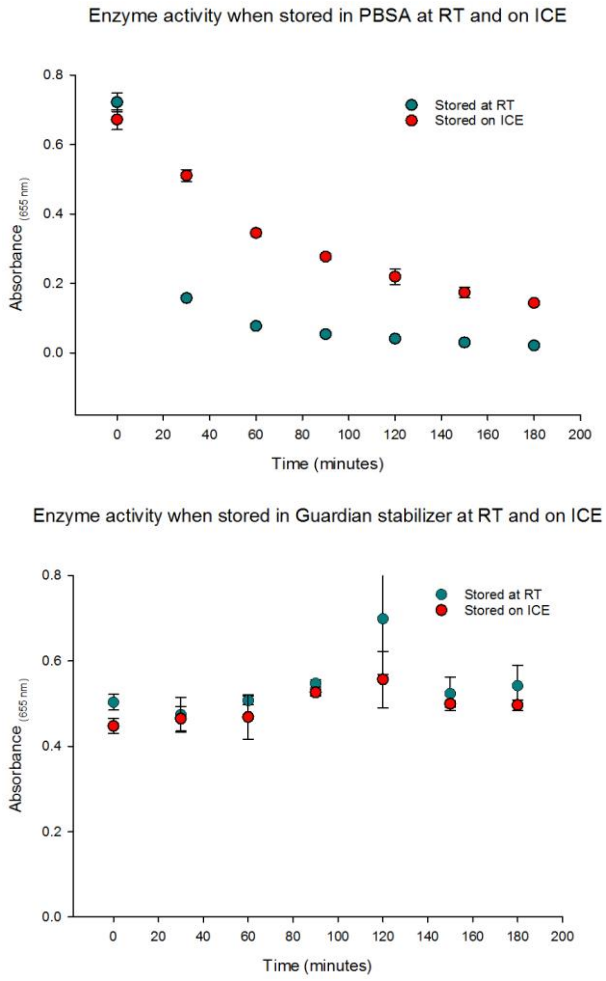

Figure 14. Stability study of HRP at room temperature and on ice. Enzyme tagged to antibody was mixed in 0.1% PBSA and Guardian buffer in 2 replicates each. Stability of enzyme that was stored at RT declined with increase in time with up to more than 90% loss but samples mixed in guardian stabilizer were stable at RT or on ice.

Spectral analysis of GB (absorption spectra): In order to work with guardian buffer in inline filter assays, it was important to know the wavelength at which a sample in guardian buffer absorbs and emits light. An antibody concentration of 800 ng/ml prepared in 0.1% PBSA and Guardian buffer (in 2x replicates each) was incubated with TMB and read for spectral scans. Spectral scan of antibody in PBSA and Guardian buffer indicated that the sample in PBSA and Guardian buffer had a peak at 655 and 450 nm resp (Figure 15 i, ii). Spectral scans for antibody concentrations of 200, 400 and 800 ng/ml in GB confirms emission peak at 450 nm (figures not shown). The guardian buffer has a yellow color by itself (absorbs from 420 to 490 nm), which in the presence of HRP and TMB turns into a bluish-green color (absorbs 450 nm and again between 550-600 nm), with maximum absorbance at 450 nm (λ_{max}), see Figure 15. Therefore, colorimetric assays further performed in guardian buffer were read for absorbance at 450nm.

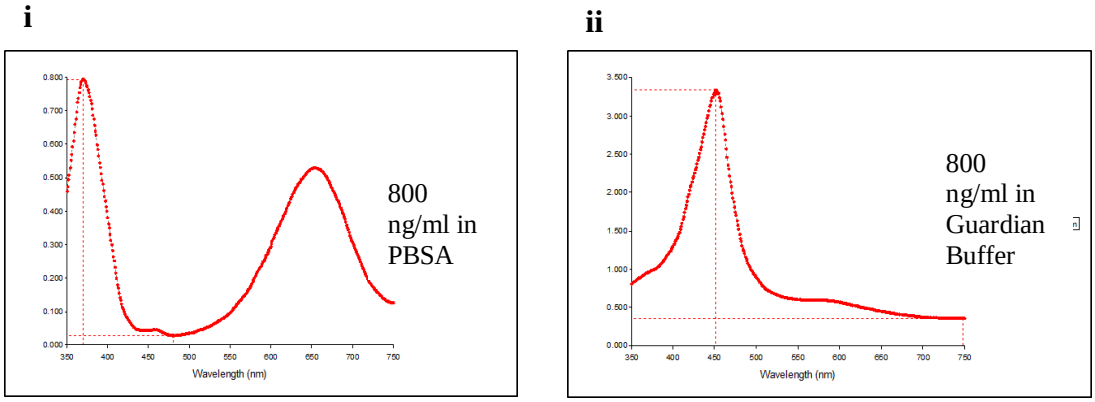

Figure 15. Spectral analysis of Guardian buffer. Absorption spectra for anti-crypto-HRP in Guardian buffer. Panel A shows absorption spectra of the antibody in two different buffers, 0.1% PBSA (i) and Guardian buffer (ii). Panel B shows absorption spectra in Guardian buffer at different antibody concentrations

The HRP enzyme was more stable in guardian buffer at room temperature than in PBSA therefore all 3-D assays were further performed using guardian stabilizer diluent as buffer when HRP tagged antibody was used.

Enzyme Retention Assay using Inline Filter Holder: Guardian buffer

Initial experiments to determine the cause of non-specific signal in 3-D enzyme retention assays lead to identifying loss of enzyme stability and characterization of Guardian buffer, another enzyme retention assay was performed using inline filter holder at different concentrations of cryptosporidium oocysts (see methods). As anticipated, a decrease in absorbance intensity was seen with increasing oocyst concentration as a result of depletion of enzyme-bound pathogen by cellulose acetate (Figure XX). This assay was also performed at other antibody concentrations which did not yield desired results (not shown here).

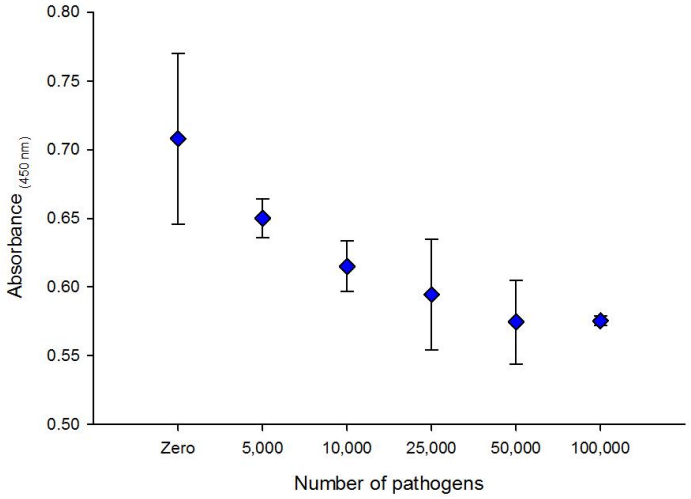

Figure 16. *Cryptosporidium* concentration series in Guardian buffer using in-line filter 3-D enzyme retention assay. Flow through from a range of *Cryptosporidium* oocysts at varying concentrations that were passed through cellulose acetate were read for its absorbance at 450 nm and plotted. A decrease in absorbance intensity was observed with increasing oocyst conc. suggesting that the oocyst and its bound HRP-antibody were depleted.

Double-sided Adhesive: Strength and Wettability

A simple test was done to determine the strength and wettability of a double-sided adhesive used in 3-D paper devices that holds cellulose acetate filter. Two assembled 3-D devices, one dry and other wet with buffer, was pulled apart and was observed for any overflow of the buffer using tweezers to peel the double-sided adhesive that was in contact with cellulose acetate. When dry, cellulose acetate was ripped off along with adhesive but when wet there was no damaged done to the filter therefore, an adhesive- that has better adhesion to wet substances was needed.

Cryptosporidium Concentration Series in Dual Pathway 3-D Paper-based Devices: using 3M 9500 double-sided adhesive

Since the overall goal was to eliminate the use of pre-labeling technique with centrifugation using 3-D paper-based enzyme retention assay, dual pathway 3-D devices

were printed, heated and assembled, as described above, with cellulose acetate using 3M double-sided adhesive. A series of Pre-labeled prewashed *Cryptosporidium* oocysts in Guardian buffer was added to devices. When inspected visually, colorimetric signal was observed only in the device with 50,000 oocysts with similar color intensity in both C and T zone (Figure 17). This assay was not further analyzed using ImageJ.

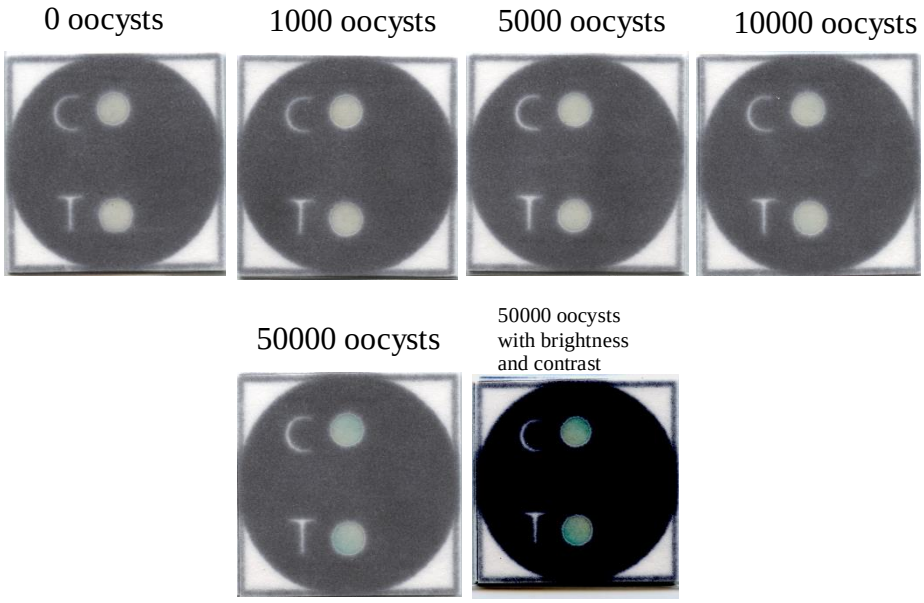

Figure 17. Pre-labeled *Cryptosporidium* concentration series in 3-D enzyme retention assay. *Cryptosporidium* concentration series using pre-labeled prewashed oocysts in dual pathway 3-D paper-based devices. All devices were scanned with no enhancement except for 50,000 oocyst device that was scanned with no enhancement and also with brightness and contrast (see methods)

Similar signal intensity was observed between T and C zones regardless of the presence or absence of pathogen when various antibody concentrations were tested at constant pathogen levels in dual pathway 3-D devices (Figure 18).

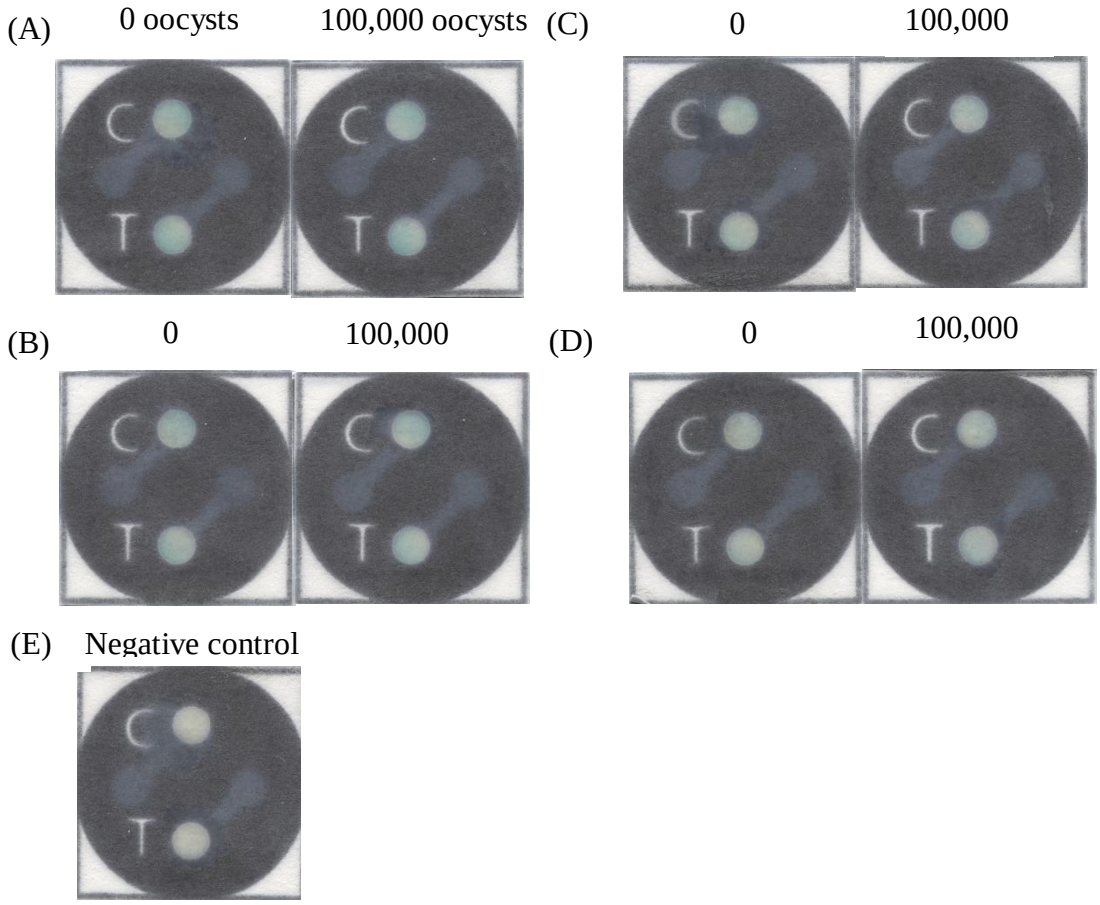

Figure 18. Antibody concentration series in 3-D devices with constant oocyst concentration. A- 1:25,000 (80 ng/ml), B-1:50,000 (40 ng/ml), C- 1:75,000 (26.66 ng/ml), D- 1:100,000 (20 ng/ml) and E- Control (no antibody, no oocysts). No visible color difference was seen between the test and control zones irrespective of oocyst concentreation

Sensitivity of the Enzymatic Assays in Paper Devices

The overall goal was to develop a paper-based microfluidic test with a visual read-out, so it was important to examine the minimum antibody-HRP concentrations that could be distinguished by the naked eye. Five devices with nine circular zones about the size of a reaction/test zone was patterned as described above. Each zone was spotted with an anti-Crypto/HRP antibody concentration ranging from 18.9 ng/ml to 200 ng/ml in 5 µl of GB and allowed to react with embedded TMB reagent (Figure 19).

Visually, no difference was apparent in the intensity of color developed at antibody concentrations between 200 ng/ml and 100 ng/ml, while a slight decline could be seen between 100 ng/ml and 50 ng/ml, followed by another decline from 50 ng/ml to 25 ng/ml (Figure 19). Small changes in antibody/HRP concentration, such as that found between roughly 30 – 40 ng/ml, could not be readily discerned with the naked eye (Figure 19, row 3). The reaction zones for each antibody concentration were then quantified, as described above, using ImageJ with a single ROI chosen that covered entire reaction zone. A scatter plot of the greyscale intensities across the full range of antibody concentrations is shown in Figure 20, left panel, while a subset of the data is shown in Figure 20, right panel, and Table 6. The intensity appeared to saturate at approximately 100 ng/ml, while the large standard deviations made it difficult to reliably detect small changes in antibody/HRP concentration.

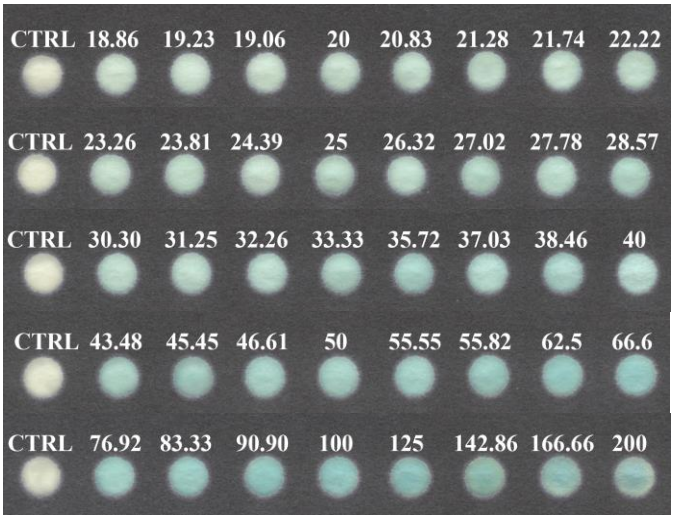

Figure 19. TMB colorimetric reaction of serially diluted HRP-antibody. Antibody spiked in to Guardian buffer was added to the circular zones pre-spotted with TMB reacted with HRP and developed a blue color based on the concentration of antibody (ng/ml) in each sample. Control was spotted with Guardian buffer only.

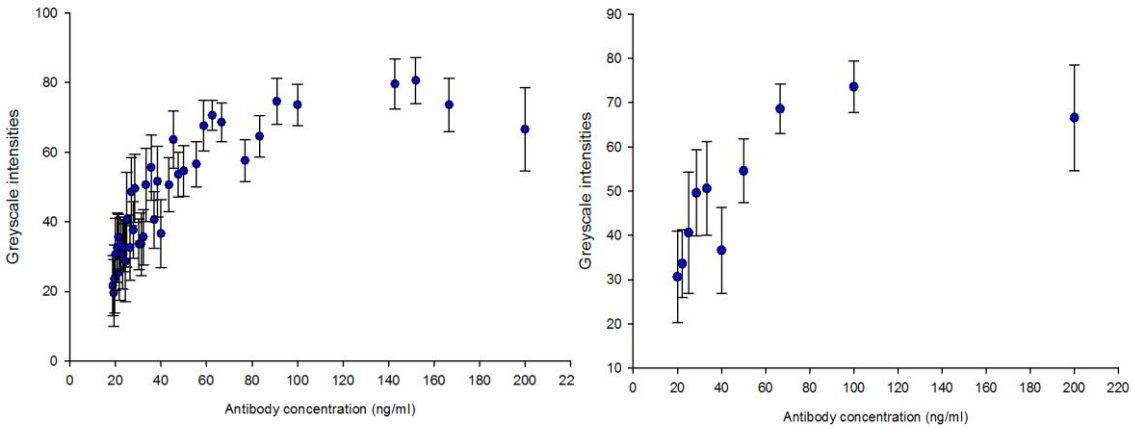

Figure 20. Scatter plot of antibody/HRP concentration-dependent colorimetric reaction in wax printed paper reaction wells. The paper devices shown in Figure 19 were scanned and the color development at each concentration of antibody was quantitated using ImageJ. An increase in color intensity was seen with increasing antibody/HRP concentration but reached saturation after roughly 100 ng/ml antibody/HRP. The scatter plot on the right shows a subset of intensities in order to clearly visualize the trend in reaction intensity.

Table 6. ImageJ quantified colorimetric signal from serially diluted HRP-antibody in paper

Antibody concentration(ng/ml)	Intensity	Standard Deviation
200	66.6	11.93
100	73.6	5.87
66.6	68.6	5.61
50	54.6	7.22
40	36.6	9.68
33.33	50.6	10.58
28.57	49.6	9.75
25	40.6	13.68
22.22	33.6	7.71
20	30.6	10.35

IV. DISCUSSION

The goal of this project was to develop paper-based devices to detect *Cryptosporidium* and *Giardia* two protozoan pathogens that cause persistent diarrhea (see introduction). Wax patterned paper devices were characterized and 2-D and 3-D devices were designed such that *Cryptosporidium* and *Giardia* could be detected together on a single device. In the 2-D multiplex design, a minimum of 250 *Cryptosporidium* oocysts and 5000 *Giardia* cysts were required to elicit a positive colorimetric signal detectable with the naked eye. These detection limits are comparable to existing detection methods [11]; although, sample concentration and isolation will likely be needed in order to reduce clinical sample volumes (>1 ml or g of stool) to the level required for the paper-based assays (typically $\leq$50 µl). In addition, the wide inter- and intra-assay variability seen in these assays could be attributed to the non-homogenous nature of the fibrous paper material such that local variations in porosity or opacity could impact color appearance or reaction development. This variation indicates that true quantitative analysis (number of pathogens extrapolated from a standard curve) may not be possible in the 2-D paper device. However, it also suggests that the use of internal controls within the same device/assay is critical for accurate positive/negative confirmation of *Cryptosporidium* oocysts.

The 3-D devices (single and dual pathway) were designed to eliminate the need for centrifugal washing to remove unbound antibodies as required in 2-D paper assays.

Here, positive pathogen detection was based upon a decrease in HRP enzyme reaching the TMB reaction zone, through the retention of enzyme-bound pathogens on a size-selective membrane. Cellulose acetate (1.2 µm) was demonstrated to successfully retain nearly all *Cryptosporidium* oocysts, which fits well with previous reports using filtration-based techniques to detect *Cryptosporidium* and *Giardia* pathogens in water sources [98]. Unfortunately, initial attempts to detect the amount of unbound antibodies reaching the end T and C zones using a 3-D dual pathway enzyme retention assay was unsuccessful with the use of both pre-labeled unwashed and pre-labeled prewashed oocyst samples. Both T and C zones turned blue, indicating similar amounts of HRP enzyme present in both pathways with/without size-selective membrane in place. This non-specific signal generation could be attributed to disassociation of HRP-antibody from pathogens due to shear forces associated with capillary flow through the fibrous paper, residual peroxide from bleaching or processing of the filter materials by the manufacturer, or possibly even poor wet-strength adhesion between the paper/membrane using double-sided adhesives that allowed oocysts to bypass the membrane all together. Follow-up experiments were performed to isolate the cause of the non-specific reaction, including enzyme retention assays with an in-line filter assembly in place of the paper substrate and recovery of lost enzyme activity with guardian stabilizer/buffer.

Examination of the paper/membrane materials and buffer components indicated a wide range of variability in % recovery of the HRP activity (from 70% to well over 100%) and that the addition of tween-20 helped to reduce these fluctuations across all materials, presumably by reducing non-specific binding of the protein (HRP-antibody) to

the paper or filter material. These studies also suggest that non-specific binding is not the likely source of false positive signal seen in 3-D enzyme retention assays.

Next, the enzyme retention assay approach was tested using an in-line filter assembly where there was no possible interference from double-sided adhesive or chromatography filter paper. When pre-labeled unwashed oocyst samples were added to filter holder containing a cellulose acetate membrane capable of retaining oocysts and its bound antibodies, an increase in absorbance intensity was seen at increasing oocyst concentrations, contrary to what was expected with the enzyme retention approach. It was also observed that the absorbance values reflecting HRP enzyme activity were far below 0.1 OD which suggested some loss of enzyme activity compared to previous experiments with the in-line assembly. Furthermore, this particular set of experiments was performed in triplicate at room temperature starting with the lowest to highest oocysts concentration, taking about 4 hours to complete the entire series. This long time period at room temperature clashes with the recommended storage conditions (4˚C) from the vendor for the enzyme-tagged antibody, which could explain loss of enzyme activity over the course of the experiment. Thus, a stability study for HRP in PBSA and a HRP stabilizer (Guardian buffer) at RT and on ice was performed and revealed that there was about 75% loss of enzyme activity in only 30 minutes when the antibody was diluted in PBSA and stored at either RT or on ice. Use of the Guardian buffer helped to maintained activity for up to 3 hrs. in order to complete this portion of the study. When the in-line filter enzyme retention assay was performed in Guardian buffer a decrease in absorbance at 655 nm was seen with increasing pathogen concentrations providing proof-of-concept for the enzyme retention assay approach and overall concept.

However, the goal was to develop a paper-based assay, so two double-sided tapes were investigated for their adhesion strength by wetting an embedded filter between adhesive and the trying to peel it off. Empirically, the 3M 5900 adhesive seemed to maintain a tight seal between the cellulose acetate filter and paper versus a generic brand that lifted off the cellulose acetate filter without much effort or damage to the membrane suggesting a lower quality seal. Unfortunately, even with these modifications the 3-D paper-based enzyme retention assay yielded no visible difference in color intensity between the T and C zones, even when using prewashed oocyst samples. Our current working theory, which will be followed up in future work, is that the shear forces encountered during fluid flow in the paper are causing rapidly disassociation of the antibody:oocysts complexes releasing free antibody that can reach the reaction zone.

These lackluster results lead us to ask the question "what is the minimum change in HRP-antibody concentration that can be visibly detected using the colorimetric TMB reaction in paper?" Serial dilutions of HRP-antibody reacted with TMB spotted paper zones demonstrated that it takes a relatively large change in antibody concentration to visibly alter the enzymatic color reaction. In general, the antibody/HRP concentration had to more than double before a clear visual or quantitative difference in color reaction could be detected, for example from 20 ng/ml to 50 ng/ml, which represents a difference of approximately 1.5×10^9 antibody/HRP molecules (estimated MW of 326,000 g/mol; IgG ~150 kDa and HRP ~44 kDa at 1:4 ratio in 20 µl volume). In terms of detection using the enzyme retention concept, if we meet the LOD for microscopy (10^5 pathogens/ml) and assume a 100:1 binding ratio of antibodies per pathogen in a concentrated stool sample, then only 10^7 antibody/HRP molecules could theoretically be depleted from the bulk

antibody solution, two orders of magnitude less than what was required to elicit a visible change. Even to yield a yes/no binary result, it is unlikely that a sufficient number of HRP-antibody molecules would be bound to *Cryptosporidium* oocysts and depleted from the bulk antibody solution in order to affect the visible color intensity during an assay. This suggests that the TMB colorimetric assay in paper has limited sensitivity for pathogen detection using the enzyme retention approach. Alternative approaches are currently being explored that follow more conventional sandwich-based immunoassay formats to immobilize pathogens within specific regions of the paper-based microfluidic devices for spatial localization and detection of a signal that is directly proportional to the number of oocysts present in a sample.

LITERATURE CITED

1. Liu, L., H.L. Johnson, S. Cousens, J. Perin, S. Scott, J.E. Lawn, I. Rudan, H. Campbell, R. Cibulskis, M. Li, et al., *Global, regional, and national causes of child mortality: an updated systematic analysis for 2010 with time trends since 2000.* Lancet, 2012. **379**(9832): p. 2151-61.
2. Lozano, R., M. Naghavi, K. Foreman, S. Lim, K. Shibuya, V. Aboyans, J. Abraham, T. Adair, R. Aggarwal, S.Y. Ahn, et al., *Global and regional mortality from 235 causes of death for 20 age groups in 1990 and 2010: a systematic analysis for the Global Burden of Disease Study 2010.* Lancet, 2012. **380**(9859): p. 2095-128.
3. Lima, A.A., S.R. Moore, M.S. Barboza, Jr., A.M. Soares, M.A. Schleupner, R.D. Newman, C.L. Sears, J.P. Nataro, D.P. Fedorko, T. Wuhib, et al., *Persistent diarrhea signals a critical period of increased diarrhea burdens and nutritional shortfalls: a prospective cohort study among children in northeastern Brazil.* J Infect Dis, 2000. **181**(5): p. 1643-51.
4. Guerrant, R.L., J.B. Schorling, J.F. McAuliffe, and M.A. de Souza, *Diarrhea as a cause and an effect of malnutrition: diarrhea prevents catch-up growth and malnutrition increases diarrhea frequency and duration.* Am J Trop Med Hyg, 1992. **47**(1 Pt 2): p. 28-35.
5. Baqui, A.H., R.B. Sack, R.E. Black, H.R. Chowdhury, M. Yunus, and A.K. Siddique, *Cell-mediated immune deficiency and malnutrition are independent risk factors for persistent diarrhea in Bangladeshi children.* Am J Clin Nutr, 1993. **58**(4): p. 543-8.
6. Black, R.E., L.H. Allen, Z.A. Bhutta, L.E. Caulfield, M. de Onis, M. Ezzati, C. Mathers, and J. Rivera, *Maternal and child undernutrition: global and regional exposures and health consequences.* Lancet, 2008. **371**(9608): p. 243-60.
7. Black, R.E., K.H. Brown, and S. Becker, *Malnutrition is a determining factor in diarrheal duration, but not incidence, among young children in a longitudinal study in rural Bangladesh.* Am J Clin Nutr, 1984. **39**(1): p. 87-94.
8. Keusch, G.T., D.M. Thea, M. Kamenga, K. Kakanda, M. Mbala, C. Brown, and F. Davachi, *Persistent diarrhea associated with AIDS.* Acta Paediatr Suppl, 1992. **381**: p. 45-8.
9. Lima, A.A., T.M. Silva, A.M. Gifoni, L.J. Barrett, I.T. McAuliffe, Y. Bao, J.W. Fox, D.P. Fedorko, and R.L. Guerrant, *Mucosal injury and disruption of intestinal barrier function in HIV-infected individuals with and without diarrhea and cryptosporidiosis in northeast Brazil.* Am J Gastroenterol, 1997. **92**(10): p. 1861-6.
10. Ochoa, T.J., E. Salazar-Lindo, and T.G. Cleary, *Management of children with infection-associated persistent diarrhea.* Semin Pediatr Infect Dis, 2004. **15**(4): p. 229-36.
11. White, A.C., *Cryptosporidiosis (Cryptosporidium hominis, Cryptosporidium parvum and Other species),* in *Principles and Practice of Infectious Diseases*, Mandell, Bennett, and Dolin, Editors. 2010, Churchill Livingstone. p. 3547-3560.

12. Crannell, Z.A., A. Castellanos-Gonzalez, A. Irani, B. Rohrman, A.C. White, and R. Richards-Kortum, *Nucleic acid test to diagnose cryptosporidiosis: lab assessment in animal and patient specimens.* Anal Chem, 2014. **86**(5): p. 2565-71.
13. Victora, C.G., J. Bryce, O. Fontaine, and R. Monasch, *Reducing deaths from diarrhoea through oral rehydration therapy.* Bull World Health Organ, 2000. **78**(10): p. 1246-55.
14. Fayer, R. and T. Nerad, *Effects of low temperatures on viability of Cryptosporidium parvum oocysts.* Appl Environ Microbiol, 1996. **62**(4): p. 1431-3.
15. Korich, D.G., J.R. Mead, M.S. Madore, N.A. Sinclair, and C.R. Sterling, *Effects of ozone, chlorine dioxide, chlorine, and monochloramine on Cryptosporidium parvum oocyst viability.* Appl Environ Microbiol, 1990. **56**(5): p. 1423-8.
16. MacKenzie, W.R., W.L. Schell, K.A. Blair, D.G. Addiss, D.E. Peterson, N.J. Hoxie, J.J. Kazmierczak, and J.P. Davis, *Massive outbreak of waterborne cryptosporidium infection in Milwaukee, Wisconsin: recurrence of illness and risk of secondary transmission.* Clin Infect Dis, 1995. **21**(1): p. 57-62.
17. Puech, M.C., J.M. McAnulty, M. Lesjak, N. Shaw, L. Heron, and J.M. Watson, *A statewide outbreak of cryptosporidiosis in New South Wales associated with swimming at public pools.* Epidemiol Infect, 2001. **126**(3): p. 389-96.
18. Quiroz, E.S., C. Bern, J.R. MacArthur, L. Xiao, M. Fletcher, M.J. Arrowood, D.K. Shay, M.E. Levy, R.I. Glass, and A. Lal, *An outbreak of cryptosporidiosis linked to a foodhandler.* J Infect Dis, 2000. **181**(2): p. 695-700.
19. Upton, S.J. and W.L. Current, *The species of Cryptosporidium (Apicomplexa: Cryptosporidiidae) infecting mammals.* J Parasitol, 1985. **71**(5): p. 625-9.
20. Okhuysen, P.C., C.L. Chappell, J.H. Crabb, C.R. Sterling, and H.L. DuPont, *Virulence of three distinct Cryptosporidium parvum isolates for healthy adults.* J Infect Dis, 1999. **180**(4): p. 1275-81.
21. DuPont, H.L., C.L. Chappell, C.R. Sterling, P.C. Okhuysen, J.B. Rose, and W. Jakubowski, *The infectivity of Cryptosporidium parvum in healthy volunteers.* N Engl J Med, 1995. **332**(13): p. 855-9.
22. Mondal, D., R. Haque, R.B. Sack, B.D. Kirkpatrick, and W.A. Petri, Jr., *Attribution of malnutrition to cause-specific diarrheal illness: evidence from a prospective study of preschool children in Mirpur, Dhaka, Bangladesh.* Am J Trop Med Hyg, 2009. **80**(5): p. 824-6.
23. Checkley, W., L.D. Epstein, R.H. Gilman, R.E. Black, L. Cabrera, and C.R. Sterling, *Effects of Cryptosporidium parvum infection in Peruvian children: growth faltering and subsequent catch-up growth.* Am J Epidemiol, 1998. **148**(5): p. 497-506.
24. Fayer, R. and B.L. Ungar, *Cryptosporidium spp. and cryptosporidiosis.* Microbiol Rev, 1986. **50**(4): p. 458-83.
25. MacKenzie, W.R., J.J. Kazmierczak, and J.P. Davis, *An outbreak of cryptosporidiosis associated with a resort swimming pool.* Epidemiol Infect, 1995. **115**(3): p. 545-53.
26. Millard, P.S., K.F. Gensheimer, D.G. Addiss, D.M. Sosin, G.A. Beckett, A. Houck-Jankoski, and A. Hudson, *An outbreak of cryptosporidiosis from fresh-pressed apple cider.* Jama, 1994. **272**(20): p. 1592-6.

27. Sorvillo, F.J., K. Fujioka, B. Nahlen, M.P. Tormey, R. Kebabjian, and L. Mascola, *Swimming-associated cryptosporidiosis.* Am J Public Health, 1992. **82**(5): p. 742-4.
28. Smith, H.V., R.A. Nichols, and A.M. Grimason, *Cryptosporidium excystation and invasion: getting to the guts of the matter.* Trends Parasitol, 2005. **21**(3): p. 133-42.
29. Chen, X.M. and N.F. LaRusso, *Mechanisms of attachment and internalization of Cryptosporidium parvum to biliary and intestinal epithelial cells.* Gastroenterology, 2000. **118**(2): p. 368-79.
30. Johnson, J.K., J. Schmidt, H.B. Gelberg, and M.S. Kuhlenschmidt, *MICROBIAL ADHESION OF CRYPTOSPORIDIUM PARVUM SPOROZOITES: PURIFICATION OF AN INHIBITORY LIPID FROM BOVINE MUCOSA.* Journal of Parasitology, 2004. **90**(5): p. 980-990.
31. Mac Kenzie, W.R., N.J. Hoxie, M.E. Proctor, M.S. Gradus, K.A. Blair, D.E. Peterson, J.J. Kazmierczak, D.G. Addiss, K.R. Fox, J.B. Rose, et al., *A massive outbreak in Milwaukee of cryptosporidium infection transmitted through the public water supply.* N Engl J Med, 1994. **331**(3): p. 161-7.
32. Hayes, E.B., T.D. Matte, T.R. O'Brien, T.W. McKinley, G.S. Logsdon, J.B. Rose, B.L. Ungar, D.M. Word, P.F. Pinsky, M.L. Cummings, et al., *Large community outbreak of cryptosporidiosis due to contamination of a filtered public water supply.* N Engl J Med, 1989. **320**(21): p. 1372-6.
33. Heijbel, H., K. Slaine, B. Seigel, P. Wall, S.J. McNabb, W. Gibbons, and G.R. Istre, *Outbreak of diarrhea in a day care center with spread to household members: the role of Cryptosporidium.* Pediatr Infect Dis J, 1987. **6**(6): p. 532-5.
34. Craun, G.F., J.M. Brunkard, J.S. Yoder, V.A. Roberts, J. Carpenter, T. Wade, R.L. Calderon, J.M. Roberts, M.J. Beach, and S.L. Roy, *Causes of outbreaks associated with drinking water in the United States from 1971 to 2006.* Clin Microbiol Rev, 2010. **23**(3): p. 507-28.
35. Hlavsa, M.C., V.A. Roberts, A.R. Anderson, V.R. Hill, A.M. Kahler, M. Orr, L.E. Garrison, L.A. Hicks, A. Newton, E.D. Hilborn, et al., *Surveillance for waterborne disease outbreaks and other health events associated with recreational water --- United States, 2007--2008.* MMWR Surveill Summ, 2011. **60**(12): p. 1-32.
36. Yoder, J.S. and M.J. Beach, *Cryptosporidiosis surveillance--United States, 2003-2005.* MMWR Surveill Summ, 2007. **56**(7): p. 1-10.
37. Yoder, J.S., C. Harral, and M.J. Beach, *Cryptosporidiosis surveillance - United States, 2006-2008.* MMWR Surveill Summ, 2010. **59**(6): p. 1-14.
38. Yoder, J.S., R.M. Wallace, S.A. Collier, M.J. Beach, and M.C. Hlavsa, *Cryptosporidiosis surveillance--United States, 2009-2010.* MMWR Surveill Summ, 2012. **61**(5): p. 1-12.
39. Hlavsa, M.C., V.A. Roberts, A.M. Kahler, E.D. Hilborn, T.J. Wade, L.C. Backer, and J.S. Yoder, *Recreational water-associated disease outbreaks--United States, 2009-2010.* MMWR Morb Mortal Wkly Rep, 2014. **63**(1): p. 6-10.

40. Tumwine, J.K., A. Kekitiinwa, N. Nabukeera, D.E. Akiyoshi, S.M. Rich, G. Widmer, X. Feng, and S. Tzipori, *Cryptosporidium parvum in children with diarrhea in Mulago Hospital, Kampala, Uganda.* Am J Trop Med Hyg, 2003. **68**(6): p. 710-5.
41. Hojlyng, N., K. Molbak, and S. Jepsen, *Cryptosporidium spp., a frequent cause of diarrhea in Liberian children.* J Clin Microbiol, 1986. **23**(6): p. 1109-13.
42. Checkley, W., R.H. Gilman, L.D. Epstein, M. Suarez, J.F. Diaz, L. Cabrera, R.E. Black, and C.R. Sterling, *Asymptomatic and symptomatic cryptosporidiosis: their acute effect on weight gain in Peruvian children.* Am J Epidemiol, 1997. **145**(2): p. 156-63.
43. Gatei, W., C.N. Wamae, C. Mbae, A. Waruru, E. Mulinge, T. Waithera, S.M. Gatika, S.K. Kamwati, G. Revathi, and C.A. Hart, *Cryptosporidiosis: prevalence, genotype analysis, and symptoms associated with infections in children in Kenya.* Am J Trop Med Hyg, 2006. **75**(1): p. 78-82.
44. Ajjampur, S.S., B.P. Gladstone, D. Selvapandian, J.P. Muliyil, H. Ward, and G. Kang, *Molecular and spatial epidemiology of cryptosporidiosis in children in a semiurban community in South India.* J Clin Microbiol, 2007. **45**(3): p. 915-20.
45. Das, P., S.S. Roy, K. MitraDhar, P. Dutta, M.K. Bhattacharya, A. Sen, S. Ganguly, S.K. Bhattacharya, A.A. Lal, and L. Xiao, *Molecular characterization of Cryptosporidium spp. from children in Kolkata, India.* J Clin Microbiol, 2006. **44**(11): p. 4246-9.
46. Cimerman, S., B. Cimerman, and D.S. Lewi, *Prevalence of intestinal parasitic infections in patients with acquired immunodeficiency syndrome in Brazil.* Int J Infect Dis, 1999. **3**(4): p. 203-6.
47. Buyukbaba Boral, O., H. Uysal, S. Alan, and O. Nazlican, *[Investigation of intestinal parasites in AIDS patients].* Mikrobiyol Bul, 2004. **38**(1-2): p. 121-8.
48. Henriksen, S.A. and J.F. Pohlenz, *Staining of cryptosporidia by a modified Ziehl-Neelsen technique.* Acta Vet Scand, 1981. **22**(3-4): p. 594-6.
49. Tortora, G.T., R. Malowitz, B. Mendelsohn, and E.D. Spitzer, *Rhodamine-auramine O versus Kinyoun-carbolfuchsin acid-fast stains for detection of Cryptosporidium oocysts.* Clin Lab Sci, 1992. **5**(6): p. 568-9.
50. Clavel, A., A. Arnal, E. Sanchez, M. Varea, J. Quilez, I. Ramirez, and F.J. Castillo, *Comparison of 2 centrifugation procedures in the formalin-ethyl acetate stool concentration technique for the detection of Cryptosporidium oocysts.* Int J Parasitol, 1996. **26**(6): p. 671-2.
51. McNabb, S.J., D.M. Hensel, D.F. Welch, H. Heijbel, G.L. McKee, and G.R. Istre, *Comparison of sedimentation and flotation techniques for identification of Cryptosporidium sp. oocysts in a large outbreak of human diarrhea.* J Clin Microbiol, 1985. **22**(4): p. 587-9.
52. Stibbs, H.H. and J.E. Ongerth, *Immunofluorescence detection of Cryptosporidium oocysts in fecal smears.* J Clin Microbiol, 1986. **24**(4): p. 517-21.
53. Johnston, S.P., M.M. Ballard, M.J. Beach, L. Causer, and P.P. Wilkins, *Evaluation of three commercial assays for detection of Giardia and Cryptosporidium organisms in fecal specimens.* J Clin Microbiol, 2003. **41**(2): p. 623-6.

54. Garcia, L.S., R.Y. Shimizu, S. Novak, M. Carroll, and F. Chan, *Commercial assay for detection of Giardia lamblia and Cryptosporidium parvum antigens in human fecal specimens by rapid solid-phase qualitative immunochromatography.* J Clin Microbiol, 2003. **41**(1): p. 209-12.
55. Siddons, C.A., P.A. Chapman, and B.A. Rush, *Evaluation of an enzyme immunoassay kit for detecting cryptosporidium in faeces and environmental samples.* J Clin Pathol, 1992. **45**(6): p. 479-82.
56. LeChevallier, M.W., W.D. Norton, and R.G. Lee, *Giardia and Cryptosporidium spp. in filtered drinking water supplies.* Appl Environ Microbiol, 1991. **57**(9): p. 2617-21.
57. Ungar, B.L., *Enzyme-linked immunoassay for detection of Cryptosporidium antigens in fecal specimens.* J Clin Microbiol, 1990. **28**(11): p. 2491-5.
58. Garcia, L.S. and R.Y. Shimizu, *Evaluation of nine immunoassay kits (enzyme immunoassay and direct fluorescence) for detection of Giardia lamblia and Cryptosporidium parvum in human fecal specimens.* J Clin Microbiol, 1997. **35**(6): p. 1526-9.
59. Chung, E., J.E. Aldom, R.A. Carreno, A.H. Chagla, M. Kostrzynska, H. Lee, G. Palmateer, J.T. Trevors, S. Unger, R. Xu, et al., *PCR-based quantitation of Cryptosporidium parvum in municipal water samples.* J Microbiol Methods, 1999. **38**(1-2): p. 119-30.
60. Nash, T.E., *Antigenic variation in Giardia lamblia and the host's immune response.* Philos Trans R Soc Lond B Biol Sci, 1997. **352**(1359): p. 1369-75.
61. Porter, J.D., C. Gaffney, D. Heymann, and W. Parkin, *Food-borne outbreak of Giardia lamblia.* Am J Public Health, 1990. **80**(10): p. 1259-60.
62. Joan M. Brunkard, P., P. Elizabeth Ailes, M. Virginia A. Roberts, P. Vincent Hill, D. Elizabeth D. Hilborn, M. Gunther F. Craun, M. Anu Rajasingham, 5, M. Amy Kahler, M. Laurel Garrison, D. Lauri Hicks, et al., *Surveillance for Waterborne Disease Outbreaks Associated with Drinking Water --- United States, 2007--2008.* 2011. **60(SS12)**: p. 38-68.
63. Cordingley, F.T. and G.P. Crawford, *Giardia infection causes vitamin B12 deficiency.* Aust N Z J Med, 1986. **16**(1): p. 78-9.
64. White, K.E., C.W. Hedberg, L.M. Edmonson, D.B. Jones, M.T. Osterholm, and K.L. MacDonald, *An outbreak of giardiasis in a nursing home with evidence for multiple modes of transmission.* J Infect Dis, 1989. **160**(2): p. 298-304.
65. Michele C. Hlavsa, M., M. Virginia A. Roberts, M. Ayana R. Anderson, P. Vincent R. Hill, M. Amy M. Kahler, M. Maureen Orr, M. Laurel E. Garrison, D. Lauri A. Hicks, M. Anna Newton, 4, D. Elizabeth D. Hilborn, et al., *Surveillance for Waterborne Disease Outbreaks and Other Health Events Associated with Recreational Water --- United States, 2007--2008.* 2011. **60(SS12)**: p. 1-32.
66. Rendtorff, R.C., *The experimental transmission of human intestinal protozoan parasites. II. Giardia lamblia cysts given in capsules.* Am J Hyg, 1954. **59**(2): p. 209-20.
67. Huang, D.B. and A.C. White, *An updated review on Cryptosporidium and Giardia.* Gastroenterol Clin North Am, 2006. **35**(2): p. 291-314, viii.
68. Wolfe, M.S., *Giardiasis.* Clin Microbiol Rev, 1992. **5**(1): p. 93-100.

69. Farthing, M.J., *The molecular pathogenesis of giardiasis.* J Pediatr Gastroenterol Nutr, 1997. **24**(1): p. 79-88.
70. Yoder, J.S. and M.J. Beach, *Giardiasis surveillance--United States, 2003-2005.* MMWR Surveill Summ, 2007. **56**(7): p. 11-8.
71. Yoder, J.S., J.W. Gargano, R.M. Wallace, and M.J. Beach, *Giardiasis surveillance--United States, 2009-2010.* MMWR Surveill Summ, 2012. **61**(5): p. 13-23.
72. Yoder, J.S., C. Harral, and M.J. Beach, *Giardiasis surveillance - United States, 2006-2008.* MMWR Surveill Summ, 2010. **59**(6): p. 15-25.
73. Redlinger, T., V. Corella-Barud, J. Graham, A. Galindo, R. Avitia, and V. Cardenas, *Hyperendemic Cryptosporidium and Giardia in households lacking municipal sewer and water on the United States-Mexico border.* Am J Trop Med Hyg, 2002. **66**(6): p. 794-8.
74. Dziuban, E.J., J.L. Liang, G.F. Craun, V. Hill, P.A. Yu, J. Painter, M.R. Moore, R.L. Calderon, S.L. Roy, and M.J. Beach, *Surveillance for waterborne disease and outbreaks associated with recreational water--United States, 2003-2004.* MMWR Surveill Summ, 2006. **55**(12): p. 1-30.
75. Mukhopadhyay, C., G. Wilson, D. Pradhan, and P.G. Shivananda, *Intestinal protozoal infestation profile in persistent diarrhea in children below age 5 years in western Nepal.* Southeast Asian J Trop Med Public Health, 2007. **38**(1): p. 13-9.
76. Fraser, D., R. Dagan, L. Naggan, V. Greene, J. El-On, Y. Abu-Rbiah, and R.J. Deckelbaum, *Natural history of Giardia lamblia and Cryptosporidium infections in a cohort of Israeli Bedouin infants: a study of a population in transition.* Am J Trop Med Hyg, 1997. **57**(5): p. 544-9.
77. Haque, R., D. Mondal, B.D. Kirkpatrick, S. Akther, B.M. Farr, R.B. Sack, and W.A. Petri, Jr., *Epidemiologic and clinical characteristics of acute diarrhea with emphasis on Entamoeba histolytica infections in preschool children in an urban slum of Dhaka, Bangladesh.* Am J Trop Med Hyg, 2003. **69**(4): p. 398-405.
78. Wongstitwilairoong, B., A. Srijan, O. Serichantalergs, C.D. Fukuda, P. McDaniel, L. Bodhidatta, and C.J. Mason, *Intestinal parasitic infections among pre-school children in Sangkhlaburi, Thailand.* Am J Trop Med Hyg, 2007. **76**(2): p. 345-50.
79. Angarano, G., P. Maggi, M.A. Di Bari, A.M. Larocca, P. Congedo, C. Di Bari, O. Brandonisio, and F. Chiodo, *Giardiasis in HIV: a possible role in patients with severe immune deficiency.* Eur J Epidemiol, 1997. **13**(4): p. 485-7.
80. Mank, T.G., J.O. Zaat, A.M. Deelder, J.T. van Eijk, and A.M. Polderman, *Sensitivity of microscopy versus enzyme immunoassay in the laboratory diagnosis of giardiasis.* Eur J Clin Microbiol Infect Dis, 1997. **16**(8): p. 615-9.
81. William E. Aldeen, * K. Carroll,2 A. Robison,2 M. Morrison,2 and D. Hale2, *Comparison of Nine Commercially Available Enzyme-Linked Immunosorbent Assays for Detection of Giardia lamblia in Fecal Specimens.* J Clin Microbiol., May 1998(36(5)): p. 1338–1340.
82. Myers, F.B. and L.P. Lee, *Innovations in optical microfluidic technologies for point-of-care diagnostics.* Lab Chip, 2008. **8**(12): p. 2015-31.

83. Martinez, A.W., S.T. Phillips, G.M. Whitesides, and E. Carrilho, *Diagnostics for the developing world: microfluidic paper-based analytical devices.* Anal Chem, 2010. **82**(1): p. 3-10.
84. Peeling, R.W., K.K. Holmes, D. Mabey, and A. Ronald, *Rapid tests for sexually transmitted infections (STIs): the way forward.* Sex Transm Infect, 2006. **82 Suppl 5**: p. v1-6.
85. Chin, C.D., T. Laksanasopin, Y.K. Cheung, D. Steinmiller, V. Linder, H. Parsa, J. Wang, H. Moore, R. Rouse, G. Umviligihozo, et al., *Microfluidics-based diagnostics of infectious diseases in the developing world.* Nat Med, 2011. **17**(8): p. 1015-9.
86. Cho, S., D.K. Kang, J. Choo, A.J. de Mello, and S.I. Chang, *Recent advances in microfluidic technologies for biochemistry and molecular biologys.* BMB Rep, 2011. **44**(11): p. 705-12.
87. Yang, J., C. Brooks, M.D. Estes, C.M. Hurth, and F. Zenhausern, *An integratable microfluidic cartridge for forensic swab samples lysis.* Forensic Sci Int Genet, 2014. **8**(1): p. 147-58.
88. Chin, C.D., V. Linder, and S.K. Sia, *Commercialization of microfluidic point-of-care diagnostic devices.* Lab Chip, 2012. **12**(12): p. 2118-34.
89. Sanati Nezhad, A., *Microfluidic platforms for plant cells studies.* Lab Chip, 2014. **14**(17): p. 3262-74.
90. Martinez, A.W., S.T. Phillips, M.J. Butte, and G.M. Whitesides, *Patterned paper as a platform for inexpensive, low-volume, portable bioassays.* Angew Chem Int Ed Engl, 2007. **46**(8): p. 1318-20.
91. Vella, S.J., P. Beattie, R. Cademartiri, A. Laromaine, A.W. Martinez, S.T. Phillips, K.A. Mirica, and G.M. Whitesides, *Measuring markers of liver function using a micropatterned paper device designed for blood from a fingerstick.* Anal Chem, 2012. **84**(6): p. 2883-91.
92. Lu, Y., W. Shi, L. Jiang, J. Qin, and B. Lin, *Rapid prototyping of paper-based microfluidics with wax for low-cost, portable bioassay.* Electrophoresis, 2009. **30**(9): p. 1497-500.
93. Carrilho, E., A.W. Martinez, and G.M. Whitesides, *Understanding wax printing: a simple micropatterning process for paper-based microfluidics.* Anal Chem, 2009. **81**(16): p. 7091-5.
94. Martinez, A.W., S.T. Phillips, B.J. Wiley, M. Gupta, and G.M. Whitesides, *FLASH: a rapid method for prototyping paper-based microfluidic devices.* Lab Chip, 2008. **8**(12): p. 2146-50.
95. Fenton, E.M., M.R. Mascarenas, G.P. Lopez, and S.S. Sibbett, *Multiplex lateral-flow test strips fabricated by two-dimensional shaping.* ACS Appl Mater Interfaces, 2009. **1**(1): p. 124-9.
96. Martinez, A.W., S.T. Phillips, and G.M. Whitesides, *Three-dimensional microfluidic devices fabricated in layered paper and tape.* Proc Natl Acad Sci U S A, 2008. **105**(50): p. 19606-11.
97. Schneider, C.A., W.S. Rasband, and K.W. Eliceiri, *NIH Image to ImageJ: 25 years of image analysis.* Nat Methods, 2012. **9**(7): p. 671-5.

98. Shepherd, K.M. and A.P. Wyn-Jones, *An evaluation of methods for the simultaneous detection of Cryptosporidium oocysts and Giardia cysts from water.* Appl Environ Microbiol, 1996. **62**(4): p. 1317-22.